Transport of airborne lithogenic material down through the water column in two contrasting regions of the eastern subtropical North Atlantic Ocean

Aloys J.-M. Bory, Philip Newton

GLOBAL BIOGEOCHEMICAL CYCLES, VOL. 14, NO. 1, PAGES 297-315, MARCH 2000

Transport of airborne lithogenic material down through the water column in two contrasting regions of the eastern subtropical North Atlantic Ocean

Aloys J.-M. Bory[1] and Philip P. Newton[2]

Laboratoire des Sciences du Climat et de l'Environnement, Gif-sur-Yvette, France

Abstract. Downward particle fluxes were measured using deep–moored sediment traps deployed in two regions of contrasting primary productivity levels (mesotrophic and oligotrophic) of the eastern subtropical North Atlantic Ocean. The high percentage of lithogenic material (~20-30% on average) in the particulate matter collected shows the regional significance of the atmospheric dust inputs originating from West Africa. The magnitudes of lithogenic and biogenic fluxes decrease ~5-6 and ~8-9 fold, respectively, from near the African margin (mesotrophic region) to the remote open ocean (oligotrophic region). These trophic differences seem to give rise to differences in the characteristics of the downward transport of lithogenic material. At the oligotrophic site, the relatively low and slow export of biogenic matter apparently limits and delays the removal of lithogenic particles delivered to surface waters from the atmosphere. In contrast, the higher biological activity in the mesotrophic region seems to provide persistent conditions for an efficient and faster downward transport of the deposited lithogenic particles, and the temporal variability of lithogenic fluxes largely reflects that of the atmospheric dust inputs. Thus whether the temporal variability of the exported lithogenic flux in the water column follows that of the atmospheric deposition appears to depend on the trophic status. In the mesotrophic region the oft–observed linear relationship between lithogenic and particulate organic matter (hereinafter POM) fluxes breaks down at high POM fluxes. This observation adds weight to the idea that linear relationships between POM fluxes and some candidate proxies for POM transfer cannot be assumed when POM export is large. A high mesoscale variability of biogenic, but not lithogenic, fluxes in the water column of the mesotrophic region underscores the relevance of mesoscale studies for regional estimates of export of biogenic material.

1. Introduction

Moored sediment traps have been used for several decades to investigate particulate matter transfer processes and fluxes in the ocean water column on scales varying from days to years (see *Ittekkot et al.* [1996] for review). While much of this material is autochthonous and of biogenic origin, in some regions there is a significant allochthonous lithogenic component. For example, the low–latitude North Atlantic Ocean is known to receive large atmospheric inputs of mineral particles (hereinafter dust) originating from the Sahara and Sahel (see *Prospero* [1996a, b] for review). In the absence of significant river discharge in the northwestern African margin, atmospheric inputs are unequivocally responsible for the high mineral mass accumulation rates and patterns in bottom sediments off northwest Africa (see *Rea* [1994] for review).

A recent resurgence of interest in dust has occurred, mostly because of its potential role in both oceanic and climatic processes. It has been proposed that dust inputs, by providing a source of dissolved iron to surface waters, could significantly increase biological productivity in iron–limited oceanic areas [*Martin et al.*, 1990]. The potential of additional iron to affect productivity in this way has recently been confirmed [*Behrenfeld et al.*, 1996; *Coale et al.*, 1996a, b], although the role of dust in providing bioavailable iron has yet to be established. On the other hand, dust deposited in surface waters can take up some dissolved species by sorption processes [*Krom et al.*, 1991; *Zhuang and Duce*, 1993], potentially removing essential bioavailable nutrients. It has also been suggested that mineral particles could favor the export of organic carbon to the deep ocean by increasing the ballast of sinking particles [*Ittekkot and Haake*, 1990; *Ittekkot*, 1993] or help the preservation of exported organic carbon by locking it into surface microstructures beyond the reach of chemical and biological oxidation processes [*Keil et al.*, 1994]. Dust also enhance the productivity of land ecosystems [*Swap et al.*, 1992], and their scattering properties in the atmosphere affect the radiative forcing of climate [*Li et al.*, 1996; *Tegen et al.*, 1996; *Alpert et al.*, 1998]. Moreover, on geological timescales, dust mass accumulation rates or grain sizes in bottom sediments and ice sheets can be used as paleoclimate proxies; the variability of both properties appears to be strongly influenced by the Mi-

[1]Now at Lamont-Doherty Earth Observatory of Columbia University, Palisades, New York.

[2]Also at School of Biological and Molecular Sciences, Oxford Brookes University, Headington, England.

Paper number 1999GB900098.
0886-6236/00/1999GB900098$12.00

lankovitch cycles of orbital variability, showing a close link between the dust cycle and global climate changes [*Rea*, 1994].

Lithogenic particles, being largely refractory, are also a good tracer of some aspects of the particulate matter cycle in the ocean; they can provide, for example, information on vertical transfer, resuspension, or lateral advection [*Honjo*, 1982; *Honjo et al.*, 1982a, b; *Neuer et al.*, 1997; *Lampitt et al.*, 1999]. Such particles are too small to sink independently [*Lal*, 1980] and are known to be transported by large sinking aggregates of biological origin, such as fecal pellets or marine snow, into which they are incorporated within surface and hemipelagic waters [*Dunbar and Berger*, 1981; *Krishnaswami et al.*, 1985; *Fowler and Knauer*, 1986, and references therein; *Pilskaln and Honjo*, 1987; *Buat-Ménard et al.*, 1989; *Davies and Buat-Ménard*, 1990]. Studies in the Sargasso and Mediterranean Seas have shown a close relationship between the removal of lithogenic particles from surface waters and the biological activity leading to the export of particulate matter to the deep ocean [*Deuser et al.*, 1983; *Buat-Ménard et al.*, 1989]. Such biological control has been shown to drive the temporal variability of the lithogenic particle fluxes down through the water column of these open–ocean regions where the biological activity is rather low. A proportional relationship is generally observed between Al (as a proxy for lithogenic particles) and particulate organic carbon (hereinafter POC) fluxes in the oligotrophic open–ocean water column [e.g., *Deuser et al.*, 1983; *Jickells et al.*, 1984; *Jickells et al.*, 1990]. However, taking into account the large variability of pelagic biological activity in the world ocean, and the consequently large variability of biogenic matter export, the characteristics of lithogenic particle transfer are likely to vary from one area to another. If lithogenic stocks and flux variability in the water column on short timescales (few days to years) are to be successfully interpreted in terms of water column processes and/or atmospheric inputs for instance, then it is important to better constrain the fate of mineral particles (i.e., their transfer in the water column) in the different biogeochemical provinces of the ocean.

Sediment traps have been deployed within the Eumeli (France-Joint Global Ocean Flux Study (JGOFS)) and the Biogeochemical Ocean Flux Study (BOFS, UK-JGOFS) pro-

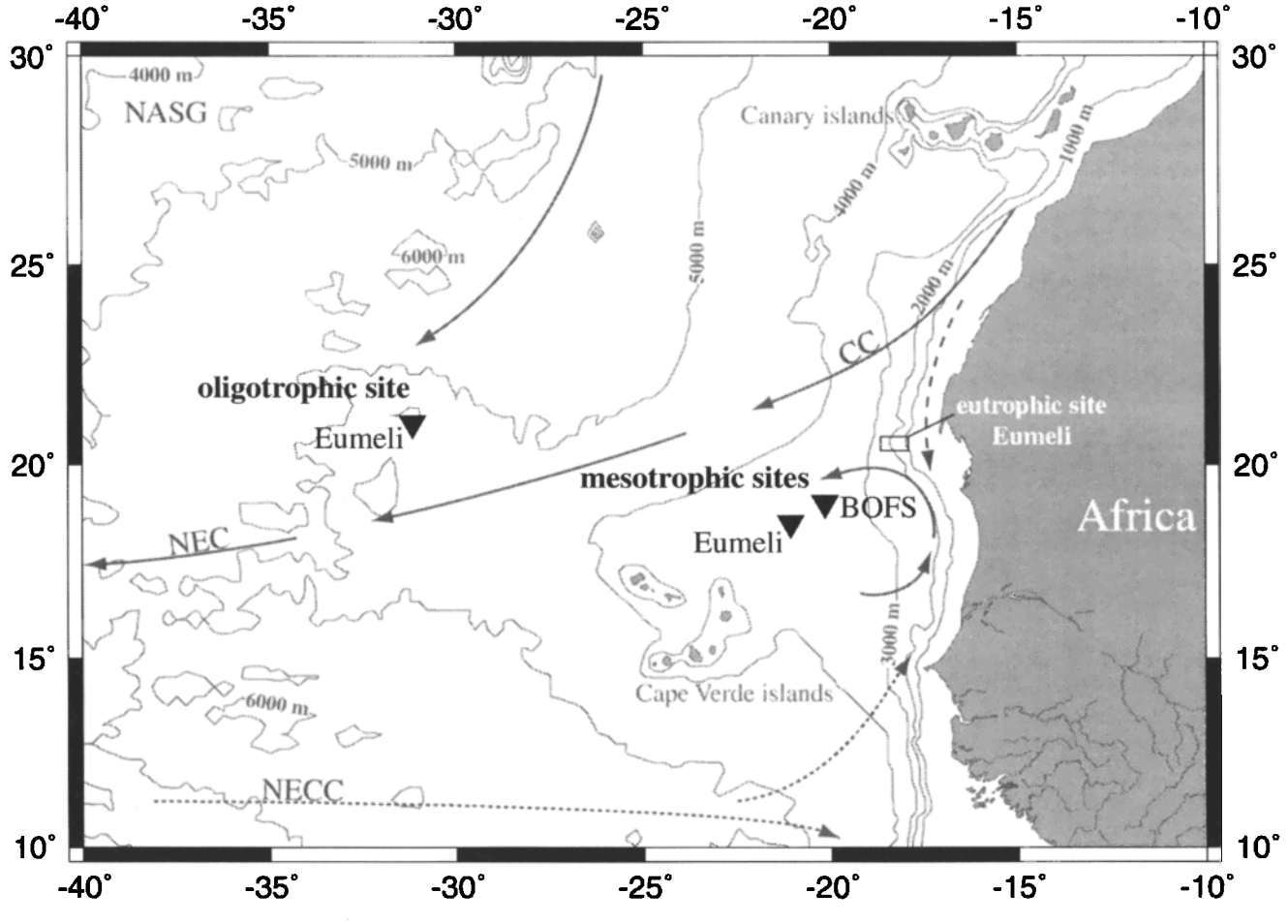

Figure 1. Mooring locations (solid triangles), bathymetry, and schematic near–surface circulation. Abreviations are CC, Canary Current; NEC, North Equatorial Current; NECC, North Equatorial Counter Current; NASG, approximate center of the North Atlantic Subtropical Gyre; BOFS, Biogeochemical Ocean Flux Study. Solid line, all year round; dashed line: fall, winter, and spring only; dotted line, summer and fall only Geographical map was obtained from M Weinelt (<http //www aquarius.geomar de/omc/>, 1999).

grammes in adjacent regions of contrasting trophic status (mesotrophic and oligotrophic) under a major atmospheric route of dust transport. This configuration (Figure 1) presents an opportunity to study the characteristics of the downward transport of dust in the water column, depending on the biological activity in the surface waters. The main objectives of this study are twofold. First, to compare, in the mesotrophic and oligotrophic regions the relationships between lithogenic and biogenic particle fluxes, from which the mechanisms of dust transfer in the water column may be assessed. Second, to discuss these results in comparing the lithogenic–particle flux variability in each ocean region and the seasonal variability of the atmospheric inputs. This study encompasses an estimation of particle flux mesoscale variability in the mesotrophic region, exploiting the proximity of two of the moorings (~100 km apart). Combined with previously published data, the results are put into the broader context of the regional variability of dust fluxes in and over the eastern subtropical and tropical North Atlantic Ocean.

2. Regional Setting

The surface waters of the study region (Figure 1), are characterized by the Canary Current (hereinafter CC) flowing southward along the African coast owing to the influence of the trade winds [*Stramma and Siedler*, 1988; *Mittelstaedt*, 1991]. The CC largely leaves the continental margin, forming the wind–driven westward North Equatorial Current (hereinafter NEC). The CC-NEC system shows a trade wind–driven seasonal variability; it weakens and shifts northward by about 5° in summer, allowing part of the eastward flowing North Equatorial Counter Current (NECC) to progress northeast toward the African coast (Figure 1). A cyclonic gyre between 15° and 21°N persists throughout the year. Below the surface waters is the Cape Verde frontal zone (between ~150 and ~600 m), where North Atlantic Central Water meets South Atlantic Central Water [*Zenk et al.*, 1991; *Pierre et al.*, 1993]. Deeper still lies another frontal zone (~22°-24°N) between Mediterranean Water and Antarctic Intermediate Water, the latter lying between ~800 and ~1000 m. Beneath this layer flows North Atlantic Deep Water (~1200-~4000 m), itself overlying Antarctic Bottom Water.

Along the northwest African coast, the upwelling of nutrient–rich waters is driven by the trade winds blowing southerly alongshore [*Mittelstaedt*, 1991]. Between 20° and 25°N, the upwelling is active all year round but is stronger in spring and late autumn; below 20°N the upwelling occurs only in winter and spring [*Speth and Detlefsen*, 1982]. Although its main impact is in shelf slope waters within ~50-60 km of the coast, its influence extends further offshore. Off Cape Blanc, for instance, giant " filaments " of cool, pigment–rich waters reach several hundred kilometers beyond the shelf break [*van Camp et al.*, 1991; *Berthon*, 1992]. The upwelling system gives rise to a strong east–to–west decreasing gradient in primary productivity; ~260 g organic C m^{-2} yr^{-1} in the mesotrophic region and ~110 g organic C m^{-2} yr^{-1} in the oligotrophic region [*Morel*, 1996], with much higher rates in eutrophic coastal waters (~535 g organic C m^{-2} yr^{-1} at the Eumeli eutrophic site; see Figure 1).

The atmospheric mineral dust particles, ranging typically from 2 to 50 μm diameter (see *Greeley and Iversen* [1985] for review), are transported from Saharan and Sahel regions across the tropical Atlantic during episodic outbreaks occurring all year round, within latitudinally shifting corridors depending on the position of the Intertropical Convergence Zone. These corridors also vary in their westward penetration and width [*Swap et al.*, 1996; *Moulin et al.*, 1997a]. Total dust deposition is estimated to be ~220 Tg yr^{-1} in the North Atlantic Ocean, decreasing from the African margin (>30 mg m^{-2} d^{-1}) to the western subtropical Atlantic (2-12 mg m^{-2} d^{-1}) [*Duce et al.*, 1991; *Jickells et al.*, 1998]. However, very few deposition flux measurements have been reported, and estimates are not well constrained. Maximum dust concentration in the air typically varies from 10^4 μg m^{-3} over the African coast to 10^2 μg m^{-3} over Barbados and French Guyana [*Lepple and Brine*, 1976; *Prospero and Nees*, 1977; *Savoie and Prospero*, 1977]. The Cape Verde area has long been known as the " Dark Sea " because of the poor atmospheric visibility due to airborne dust [*Game*, 1964]; it is also where dust falls on ships have frequently been recorded [*Darwin*, 1846; *Ehrenberg*, 1862; *Semmelhack*, 1934; *Kuenen*, 1950]. Atmospheric dust concentrations at ground/sea level show a strong seasonal cycle, with higher values between November and April (e.g. at Sal, the northeastern island of the Cape Verde archipelago [*Chiapello et al.*, 1995]). This cycle is driven by the lower atmospheric transport occurring within the continental trade winds (Harmattan) in winter. In summer, the dust transport takes place in a higher atmospheric layer (the Saharan Air Layer (SAL)), above the trade winds inversion (they have a marine origin at this time of the year); relatively low dust concentration is seen at ground level [*Prospero and Carlson*, 1972; *Jaenicke and Schütz*, 1978; *Chiapello et al.*, 1995].

3. Materials and Methods

Settling particles at the three sites (Figure 1) were collected using conical sediment traps moored at several depths in the water column ranging from 1000 to 3190 m. Time series were obtained between 1990 and 1992 for 9 to 16 month periods (Table 1). Sampling intervals varied from 10 days (or even less for few samples) for the Eumeli traps (synchronized at all depths and between the two moorings), to 21 or 28 days for the BOFS traps (synchronized at all depths). All moorings carried current meters, which were 10 m below the traps and at ~250 m depth on the Eumeli moorings, and at 1900 m depth on the BOFS mooring. Detailed mooring configurations are described elsewhere [*Shimmield*, 1990; *Bournot et al.*, 1995].

Sediment trap sampling procedures were consistent with JGOFS protocols [*Scientific Committee on Oceanic Research*, 1990] and are fully detailed elsewhere [*Newton et al.*, 1994; *Leblond et al.*, 1995]. Sampling cups were filled prior to deployment with deep seawater from the vicinity of the mooring site mixed with a buffered formalin solution to a final concentration of 2% wt/vol formaldehyde (Eumeli and BOFS) and 5‰ excess salinity (BOFS only). After recovery a fraction of the supernatant was removed, and buffered ~40% formaldehyde was added to give a formaldehyde concentration supplement of 0.15-0.20%. Samples were refrigerated in the dark before manipulation on land. All laboratory manipulations were con-

Table 1. Average Mass Flux and Composition of Sediment trap Material

Site	Sampling Duration	Trap Depth m	Water Column Depth m	Mass Flux mg m^{-2} d^{-1}	Opal %	POM %	$CaCO_3$ %	Lithogenic %
			Oligotrophic					
Eumeli	Feb. 23, 1991 to Sept. 18, 1991	1000	4560	31.5	n.d.	12.4	58.6[a]	21.5
21°03'N, 31°10'W	Sept. 29, 1991 to May 6, 1992	1000		39.1	n.d.	10.3	58.4	27.6
	March 5, 1991 to Sept. 18, 1991	2500		34.4	n.d.	10.0	58.9[b]	25.7[b]
	Sept. 29, 1991 to May 6, 1992	2500		37.8	n.d.	8.7	59.2	30.1
	Feb. 23, 1991 to May 6, 1992[c]	1000		35.0	n.d.	11.2	58.5[a]	25.0
	March 5, 1991 to May 6, 1992[c]	2500		36.2	n.d.	9.3	59.1[b]	28.3[b]
			Mesotrophic					
Eumeli	Feb. 13, 1991 to Sept. 11, 1991	1000	3100	241	n.d.	27.0	46.5	17.2
18°30'N, 21°05'W	Feb. 13, 1991 to Sept. 13, 12991	2500		269	7.0[d]	25.0	51.3	20.1
BOFS	Oct. 21, 1990 to June 30, 1991	1140	3295	260	9.0	17.5	44.8	22.7
19°00'N, 20°10'W	Oct. 21, 1990 to May 12, 1991	2190		233	7.5	15.0	46.2	28.8
	Oct. 21, 1990 to March 30, 1991	3190		222	7.3	10.8	47.4	33.2
	Oct. 21, 1990 to March 30, 1991[e]	1140		292	9.1	14.0	46.1	25.2
	Oct. 21, 1990 to March 30, 1991[e]	2190		256	7.5	13.6	47.4	29.1
	Oct. 21, 1990 to March 30, 1991[e]	3190		222	7.3	10.8	47.4	33.2

Sediment traps used were Technicap PPS-5 (Eumeli) and Parflux Mark 7G-13 (BOFS) whose aspect ratios (i.e., height/diameter ratio) are 1.54 and 1.30, respectively; the former has a sampling aperture of 1 m^2 covered with honeycomb baffle of 1 cm diameter/5 cm depth, and the latter has a collection area of 0.5 m^2 also fitted with a honeycomb baffle but of 2.5 cm diameter/6.25 depth cells [*Honjo and Doherty*, 1988]. Abreviation n.d., no data.

[a] One sample is missing (corresponding sampling period: Aug. 22, 1991 to Sept. 1, 1991).

[b] Four samples are missing (corresponding sampling periods: March 5, 1991 to March 15, 1991 and March 25, 1991 to April 24, 1991).

[c] No sampling during the Sept. 18, 1991 to Sept. 28, 1991 period (mooring recovery and re-deployment time).

[d] Sampling period reduced to Feb. 13, 1991 to Sept. 11, 1991.

[e] Sampling period common to all three BOFS traps.

ducted in filtered air environments using trace–metal–clean procedures. Swimmers were identified and removed according to the criteria of *Knauer and Asper* [1989] and *Michaels et al.* [1990]; this step was preceded by sieving through a 1 mm nylon mesh for the Eumeli samples. Splitting into subsamples was carried out by established methods (Eumeli [*Heussner et al.*, 1990] and BOFS [*Honjo*, 1978]).

Mass flux was obtained by weighing several subsamples filtered onto preweighed polycarbonate membrane filters (0.4 μm porosity), immediately rinsed with isotonic (0.56 N) ammonium formate to remove salt and excess formalin, and dried at ~40°C (bar Eumeli subsamples analyzed for organic carbon and opal, which were rinsed in deionized water, centrifuged, and lyophilized). For elemental analyses the particle cake was removed from the filter by peeling.

Organic carbon content was determined by combustion and detection of liberated CO_2 (for details, see *Newton et al.* [1994] for BOFS and *Legeleux* [1994] for Eumeli). Particulate organic matter (POM) content was calculated as twice the POC content. Opal content was measured for all BOFS samples [*Jickells et al.*, 1996] and for one Eumeli time series [*Ballouey*, 1994] using methods based on those of *Mortlock and Froelich* [1989].

Al, Ca, Ti, Fe, and Ba concentrations were measured by inductively coupled plasma - atomic emission spectrometry (ICP-AES). Between ~10 and ~100 mg of sediment trap material were totally dissolved using an ultrapure HNO_3/HCl/HF (4.5/1.5/4) mixture in Teflon bombs using a microwave heating system [*Bory*, 1997] and diluted with ~2% vol/vol HNO_3 solution for analysis. Blanks were determined (at least one per five samples) to check for contamination during the preparatory and analytical procedures. The accuracy of the complete dissolution and analytical method was tested using analyses of a geological sediment standard (BCSS-1, National Research Council of Canada). Precision of the entire preparatory and analytical procedures was established by replicates.

Lithogenic content was estimated from Al concentration, assuming that lithogenic material is 8.4% Al [*Turekian and Wedepohl*, 1961]. In support of this approach, Ti and Fe, which are also crustal tracers [*Taylor and McLennan*, 1985], were linearly correlated to Al, and Ti/Al and Fe/Al ratios (0.066±0.002 (1σ) and 0.54±0.02, respectively) were similar to those of *Vinogradov* [1959] and *Bowen* [1966] for soils (0.065-0.070 and 0.53-0.54, respectively) [*Bory*, 1997]. Moreover, the Fe/Al ratio was similar to that in atmospheric dust over the same region (0.514-0.542, depending on the source regions [*Chiapello*, 1996]). Carbonate content was calculated from Ca concentration in the samples as $CaCO_3$; Mg–calcite is estimated to be negligible [*Newton et al.*, 1994], as is lithogenic Ca (based on Ca/Al (0.2-0.6) in dust collected at Sal [*Chiapello*, 1996] and the likelihood of incomplete dissolution).

4. Results

4.1. Sampling Artefacts

The measurement of current speed provides a check on the likelihood of a significant hydrodynamic bias compromising sample collection. The overall average current speed during Eumeli mooring deployments was <6 cm s^{-1} at 1000 m and <4 cm s^{-1} at 2500 m [*Bournot et al.*, 1995]. Most of the 1–hour–average current speeds at 1000 m, and all of them at 2500 m, were <15 cm s^{-1}, as well as at the BOFS site (always <~9 cm s^{-1}, at 1900 m). Currents of this magnitude are unlikely to cause major hydrodynamic bias to trap collection of fast–settling particles for bottom–moored traps of this geometry and design [*Baker et al.*, 1988; *Honjo and Doherty*, 1988; *Knauer and Asper*, 1989; *Bacon*, 1996]. For 12 sampling periods (Eumeli), speeds >15 cm s^{-1} were recorded at 1000 m but never exceeded 20 cm s^{-1}. During 10 of these, the 15 cm s^{-1} threshold was exceeded for <4% of the time, and for the other two (one at the mesotrophic site, one at the oligotrophic site) the threshold was exceeded for ~10% of the time. One of these latter two periods, which is also when the highest speed is recorded, coincides with an unusual decrease in mass flux at 1000 m relative to 2500 m. No other correlation is evident between current speed and particle flux, giving some confidence in the quality of the flux data. This confidence is reinforced for all sites by the clear consistency between flux time series recorded at different depths despite changing hydrodynamic conditions with depth. Mean horizontal currents (Eumeli) have a marked westward component at all depths and are generally flowing southwest [*Bournot et al.*, 1995]. Identified and removed swimmers were present at levels of less than a few percent of the particle fluxes reported here. At such levels, swimmer–related artefacts, further minimized by the use of formaldehyde in the sampling cups, are likely to be negligible.

4.2. Material Fluxes and Settling Rates

4.2.1. Oligotrophic site. Mass flux is ~35 mg m^{-2} d^{-1} on average at both 1000 and 2500 m over the 15–month sampling period (Table 1), showing variability but no marked seasonal trend (Figure 2a). Time series at the two depths are generally similar, but the flux is usually higher at 1000 m during periods of increasing flux and higher at 2500 m as fluxes decrease. This apparent time lag between flux events at the two depths, the main peaks actually occur about one sampling period (i.e., 10 days) later at 2500 m, allows the estimation of a settling rate of ~150 m d^{-1}.

The fluxes of POM, $CaCO_3$ and lithogenic material closely follow the mass flux pattern at both depths; only those at 1000 m are shown (Figure 2b) as data from 2500 m show similar trends. $CaCO_3$, and to a lesser extent the lithogenic material, largely dominate the relatively steady composition (Figure 2b). No large changes in the composition are observed between the two depths (Table 1). The undetermined fraction (total - {$CaCO_3$ + lithogenic + POM}), presumably biogenic opal, is ~5-6% and ~3-4%, on average, of the content at 1000 and 2500 m, respectively (these two ranges are significantly different at the probability threshold of 1%). Lithogenic fluxes are on average 8.8 and 10.2 mg m^{-2} d^{-1} at 1000 and 2500 m, respectively.

4.2.2. Mesotrophic sites, Eumeli. The average mass flux is ~7-8 times higher than at the oligotrophic site at a given depth (Table 1). Mass flux at 1000 m ranges from ~20 to 750 mg m^{-2} d^{-1} (Figure 3a), showing a much higher absolute and relative variability than at the oligotrophic site (Figure 3b). The mass flux time-series at 1000 and 2500 m depth are similar (Figure 3, a), especially during the peaks. As at the oligotrophic site, the flux tends to be larger at 1000 m at the beginning of the peaks, and larger at 2500 m at the end of

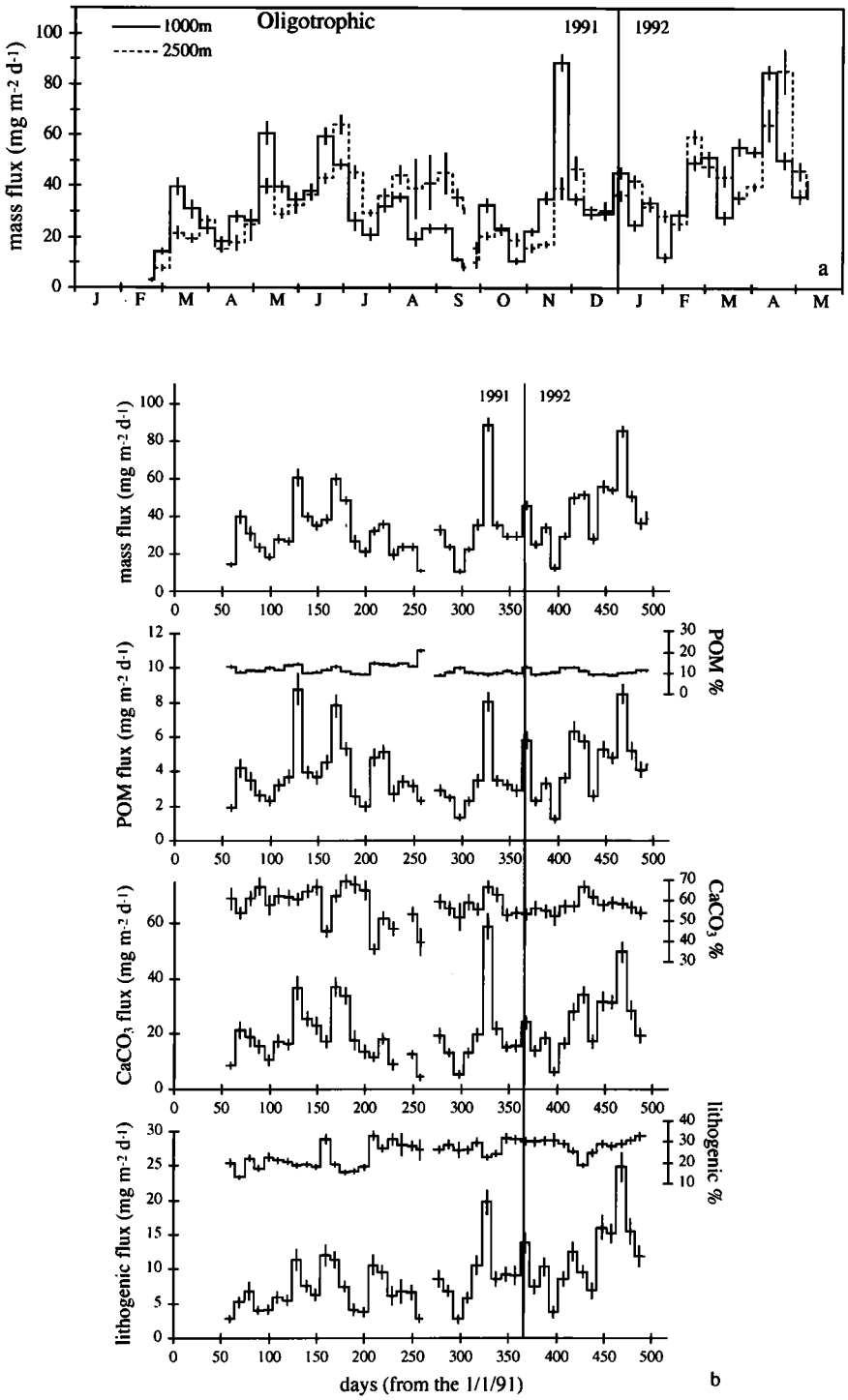

Figure 2. Temporal variability of (a) mass flux at 1000 and 2500 m and (b) mass, POM, $CaCO_3$, and lithogenic fluxes and contents at 1000 m, at the Eumeli oligotrophic site. Sub-sampling errors were estimated as the standard deviation on subsample mass determinations (1σ). Fractional errors on POM analyses were estimated to be 3% (H. Etcheber, personal communication, 1997). Errors on carbonates and lithogenic fractions include estimated uncertainties on sample weighing, dilution, and ICP-AES analysis; the latter, obtained from analyses replication, was always better than 3% (1σ). Blanks' contents were close to detection limits and negligible in all cases. BCSS-1 measurements conform to an accuracy of ±5% of the measured elements (for Ba no value is given for the standard). Standard deviations between independent replicates are all within the error bars. See *Bory* [1997] for details.

them (more clearly seen when the time series are smoothed; bottom panel of Figure 3a). However, " benchmarks " [*Honjo*, 1996] always occur within the same sampling period at both depths, indicating a much shorter time lag between flux events at 1000 and 2500 m than at the oligotrophic site. Exploiting the consistent but subtly different patterns of mass flux changes between the two depths during the main flux events, a simple model has been developed to determine the settling rates. For each of the two large peaks, a " continuous " flux signal was retrieved from the 1000 m data using the sum of 3 G functions. The continuous signal was obtained by tuning the Gauss function parameters and by comparing, using an iterative method, its integration on a 10–day–interval frame (simulating the sediment trap sampling resolution) with the 1000 m trap data until the former matched optimally the latter. It was then possible to study the changing pattern of the simulated flux due to the delay in the arrival of the flux events in the lower trap. The result of a 2 to 3–day delay best fits the 2500 m time series, allowing the estimation of a $\geq$500 m d^{-1} settling rate during these high–flux events (details given by *Bory* [1997]).

The fluxes of all the components of the particulate matter increase during the two large mass flux peaks (Figure 3b). However, in contrast to the oligotrophic site, the material is more variable in composition and, on average, much richer in POM (Table 1). $CaCO_3$ (~30-60%), POM (~10-50%), or the lithogenic fraction (~10-50%) variably dominate the particle flux (Figure 3b). Large increases in POM content, and to a lesser extent in $CaCO_3$ content, are generally observed during the major flux events; at those times, biogenic components, especially POM, dilute the lithogenic fraction. The highest lithogenic contents occur during low flux periods. Opal (only measured in the deeper trap) content is 3 to 12%; highest fluxes occur at the beginning of the major flux events. On average, particulate matter composition varies little with depth (Table 1). Lithogenic fluxes are, on average, ~5-6 times higher (41 and 54 mg m^{-2} d^{-1} at 1000 and 2500 m depths, respectively) than at the oligotrophic site during the common 7–month sampling period at the two sites.

4.2.3. Mesotrophic sites, BOFS. An artefact of unknown cause during sampling led to close–to–zero fluxes during the last two and three sampling periods at 2190 and 3190 m depth, respectively. Data from the potentially biased samples have been omitted here, based on compositional arguments presented by *Bory* [1997], and the time series shortened accordingly (Table 1). Four mass flux peaks of similar magnitude are quite evenly distributed during the deployment time (Figure 4a). The apparent relative variability of the mass flux is smaller than that of the Eumeli mesotrophic time series, but this difference could simply be a consequence of the lower time resolution of the BOFS sampling. During the common sampling period for the three BOFS traps, the time series show similar trends, but the mass flux slightly decreases with depth; at 3190 m, it is lower by ~25% on average than that at 1140 m.

At all depths, $CaCO_3$ represents the main fraction of the particulate matter; only 1140 m compositional data are shown (Figure 4b) as those from 2190 and 3190 m depth show similar trends. $CaCO_3$ and opal contents vary little in time compared to the POM or the lithogenic fraction, and their fluxes covary with mass flux. Spring mass flux events correspond to highest POM export, and the lithogenic content is generally higher when mass flux is low. Winter shows higher lithogenic contents whose fluxes peak in early 1991 and then slowly decrease until the end of the sampling time. Lithogenic fluxes are, on average, 60 to 75 mg m^{-2} d^{-1} depending on depth. Average opal and POM content decrease slightly between 1140 and 3190 m (Table 1). Conversely, there is a significant increase with depth in the lithogenic content (while $CaCO_3$ content remains almost constant).

4.3. Comparison Between Simultaneous Eumeli and BOFS Mesotrophic Records

The two mesotrophic time series cover the period February-June 1991 (1140 and 1000 m). For traps at 2190 and 2500 m the common sampling period is February-May 1991. Although the paired trap depths differ, they are sufficiently similar to allow direct comparison between the respective time series; for POM, the most labile of the main components of the settling material, expected degradation based either on a range of empirical algorithms [*Bishop*, 1989], or apparent losses observed here, is not significant compared to analytical errors. Despite BOFS and Eumeli traps and moorings not being identical, their similar geometry and design would not be expected to confer large differences in particle flux collection characteristics [*Knauer and Asper*, 1989]. Based on field study [*Honjo et*

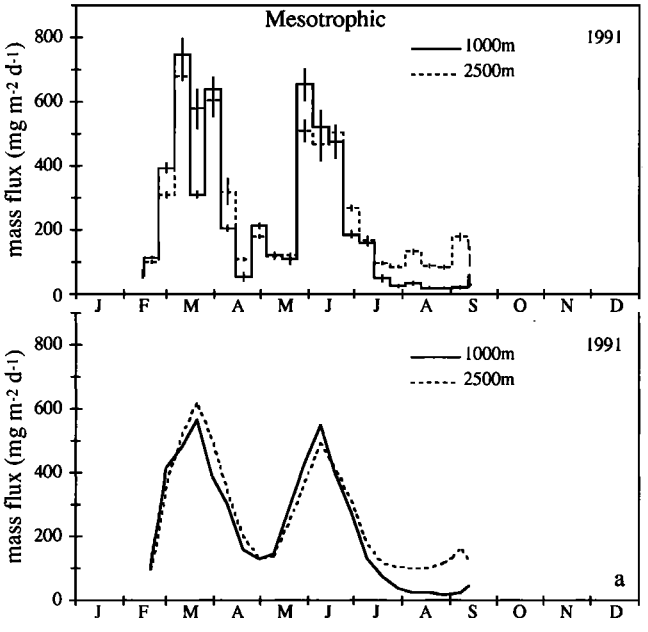

Figure 3. Temporal variability of (a) mass flux (top: raw data; bottom: the same mass flux timeseries smoothed by a three–sample running mean), and (b) mass, POM, $CaCO_3$, opal, and lithogenic fluxes and contents at 1000 and 2500 m at the Eumeli mesotrophic site. Mass and lithogenic fluxes at the oligotrophic site for the same periods and depths are also shown in Figure 3b (dashed lines). Fractional errors on opal analyses were estimated to be 3% (C. Rabouille, personal communication, 1997); errors on other analyses are as stated in Figure 2.

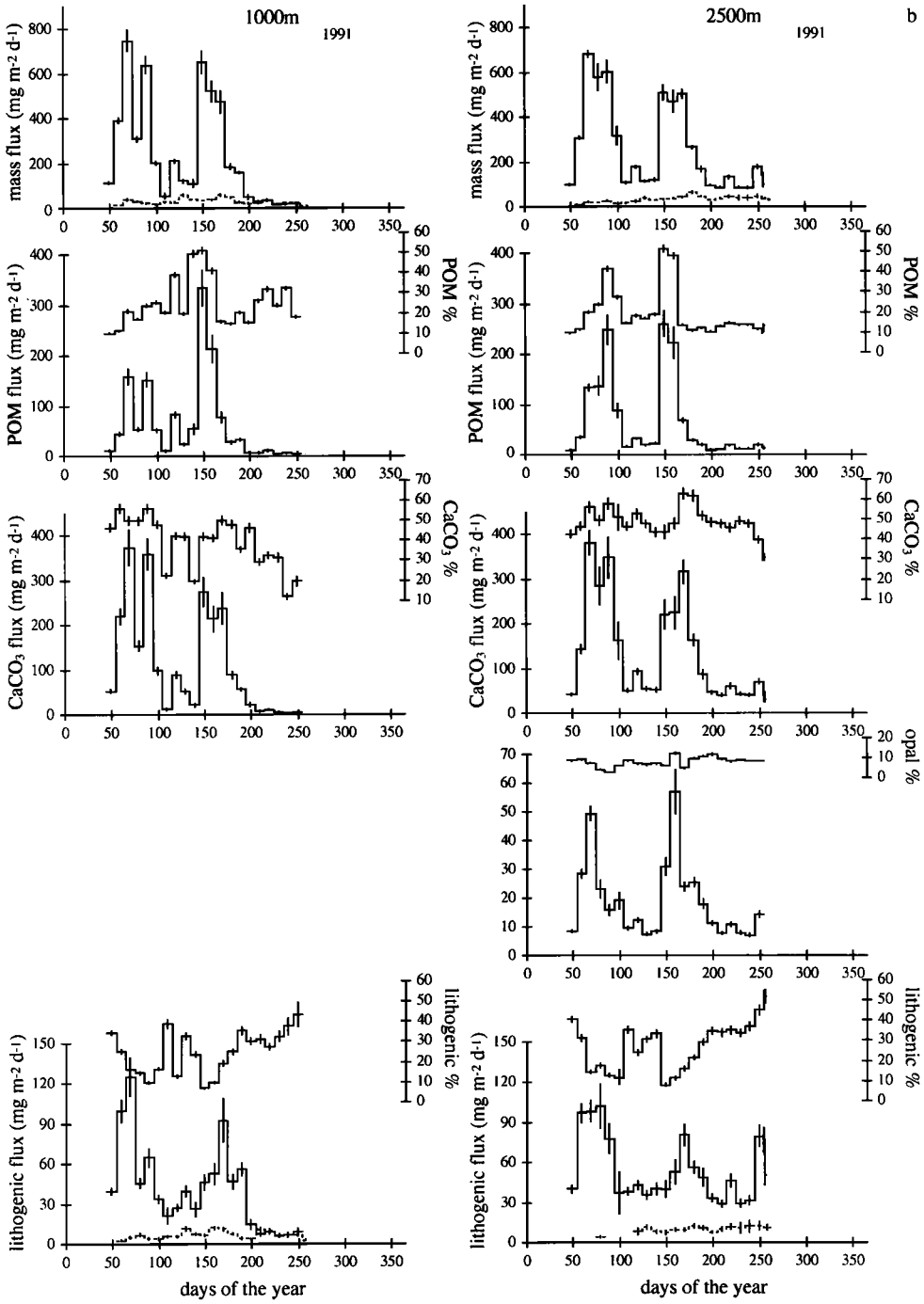

Figure 3. (continued)

al., 1992], the baffle geometry (higher depth/diameter ratio of cells of the Eumeli traps) might lead to an enhanced collection (up to 15%), but this expectation is speculative.

Figure 5 shows a comparison of the flux records. In the upper traps the period of comparison encompasses the two spring mass flux peaks observed at each site, but only the first occurs simultaneously at both sites; the second appears about a month earlier at the BOFS site. The magnitude of the peaks is higher at the Eumeli site, leading to an average mass flux at the BOFS site that is lower by ~25-30% (Table 2). For the lower traps the difference is greater because of the slight mass flux decrease with depth at the BOFS site.

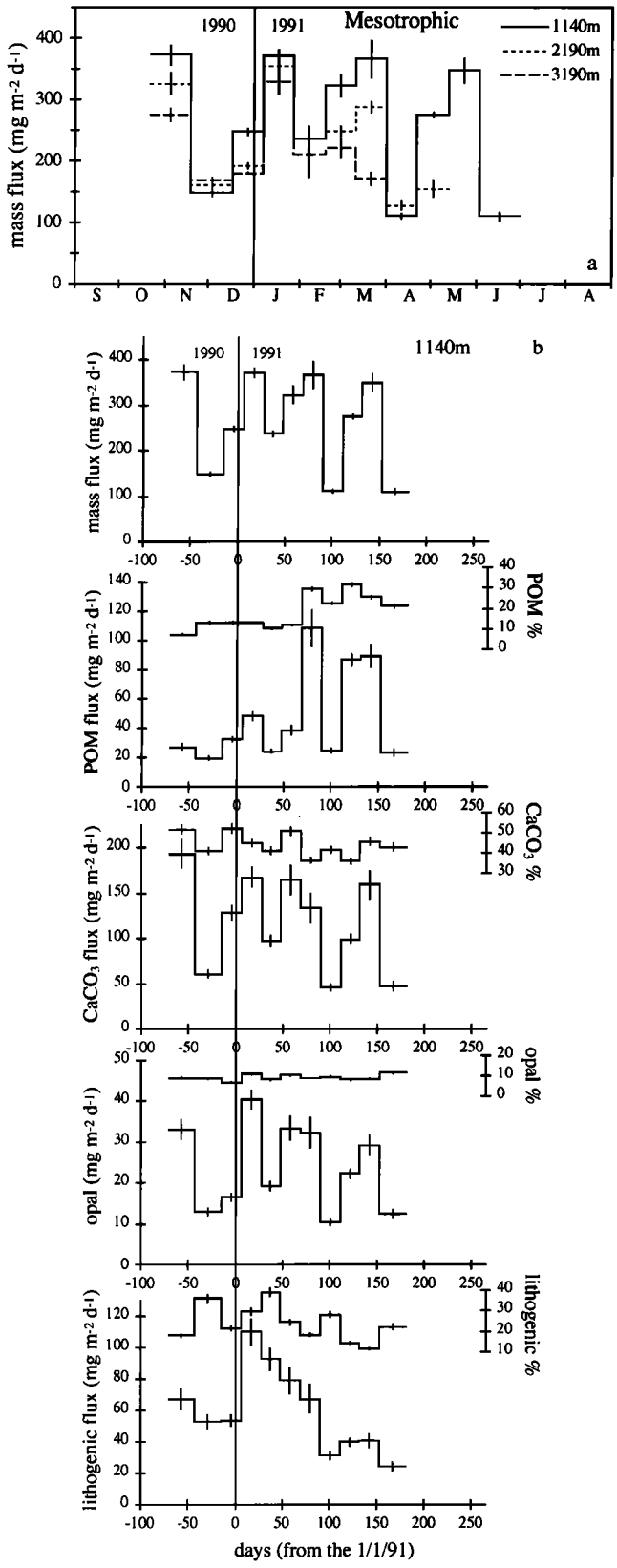

Figure 4. Temporal variability of (a) mass flux at 1140, 2190, and 3190 m and (b) mass flux, POM, $CaCO_3$, opal, and lithogenic fluxes and contents at 1140 m at the BOFS mesotrophic site. Errors on analyses are as stated in Figures 2 and 3.

Biogenic fluxes appear to account for much of the flux variability between the two sites (Table 2 and Figure 5). Average $CaCO_3$ and POM fluxes at the BOFS site represent at most 65% of the respective fluxes at the Eumeli site. Such differences are larger than analytical uncertainties (Table 2). In comparison, BOFS lithogenic fluxes are on average ~84% of the Eumeli lithogenic fluxes. Furthermore, lithogenic flux variability is in much better agreement for the two sites (r^2=0.88, upper traps) compared to biogenic components (r^2=0.28 for $CaCO_3$ and r^2=0.49 for POM). Most of the difference between the lithogenic fluxes at the upper traps of the two sites is accounted for during the last sampling period (Figure 5), with relatively low lithogenic (and biogenic) fluxes at the BOFS site.

4.4. Relationship Between Lithogenic and Organic Fluxes

There is a significant correlation between lithogenic and POM fluxes at the oligotrophic site (Figure 6a). At the mesotrophic sites, these fluxes correlate poorly (r^2=0.10 and n=32; Figure 6b). However, the two fluxes show a linear relationship for POM fluxes <~50 mg m^{-2} d^{-1} (r^2=0.80 and n=20); beyond this threshold, lithogenic fluxes are much less than expected from a linear relationship. The relatively dust-poor material (Al/POC 0.025 to 0.2) is that of the large spring flux events. Al/POC ratio decreases with time through the first event but increases during the second one owing to the time lag between POM and lithogenic flux events (Figure 7). In both mesotrophic and oligotrophic regions, similar results are obtained deeper in the water column, although they are slightly less marked because of the lower fluxes. In general, the Al/POC ratio is higher at the oligotrophic site (0.38 on average at 1000 m) compared to the mesotrophic sites (0.29 and 0.21 on average at 1140 and 1000 m, respectively), and varies inversely with POM.

4.5. Residence Time of Lithogenic Particles in Surface Waters

A few particulate aluminium (hereinafter pAl) concentration profiles were determined at the mesotrophic and oligotrophic sites in June 1992 [*Tachikawa et al.*, 1999] using samples collected by in situ filtration. Estimations of pAl residence times in the surface waters (0-200 m), where most packaging should arise, are deduced here as the pAl water column inventory for each site (0-200 m) divided by the averaged downward pAl flux at 1000 and 1140 m through the Eumeli and BOFS time series, assuming no major change in the pAl flux with depth. Despite uncertainties over the temporal representativity of the profiles (i.e., steady state needs to be assumed), these calculations provide first-order estimates of lithogenic particle residence times in surface waters of ~10 (mesotrophic) and ~40 (oligotrophic) days.

5. Discussion

5.1. Spatial gradient of lithogenic and biogenic fluxes

The high lithogenic contents of settling material at all sites show the importance of the atmospheric dust inputs onto this

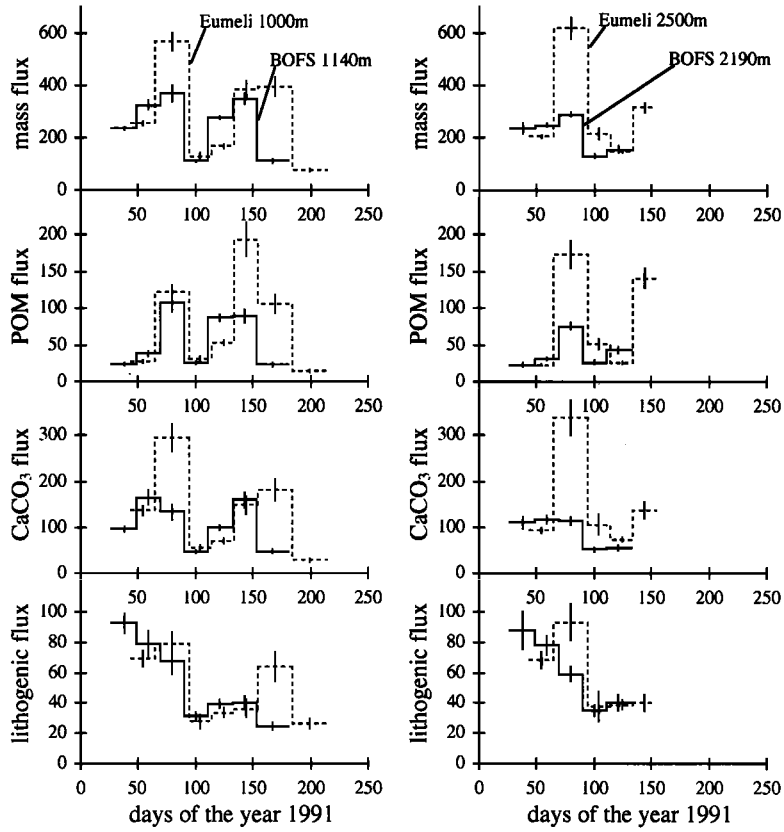

Figure 5. Comparison of mass, POM, $CaCO_3$, and lithogenic fluxes for Eumeli and BOFS mesotrophic sites at similar depths during common sampling periods. Eumeli flux data have been combined to provide a sampling resolution comparable to that of the BOFS data. Errors on analyses are stated in Figures 2 and 3.

oceanic region. Lithogenic flux decreases westward, as distance from the aeolian African dust sources increases. Average lithogenic fluxes in the mesotrophic region are among the largest (above 50 mg m^{-2} d^{-1}) recorded in the North Atlantic Ocean [*Jickells et al.*, 1996], together with those a few hundred kilometres north, off Cape Blanc [*Fischer et al.*, 1996], and south, off Cape Verde [*Ratmeyer et al.*, 1999]. The oligotrophic region receives lithogenic fluxes that are intermediate (average ~10 mg m^{-2} d^{-1}) between the mesotrophic region and the Sargasso Sea in the western subtropical North Atlantic (average ~5 mg m^{-2} d^{-1} [*Jickells et al.*, 1998]).

As expected from the progressive decrease in primary productivity moving west from the west African coast [*Morel et al.*, 1996], biogenic fluxes in the water column decrease from the mesotrophic region to the remote open–ocean oligotrophic site. POM decrease is by more than an order of magnitude between the two sites, compared to the 5-6 fold decrease for lithogenic fluxes. POM export represents a much higher frac-

Table 2. Average Mass, POM, $CaCO_3$ and Lithogenic Fluxes at Eumeli and BOFS Mesotrophic Sites During Common Sampling Periods

	Sampling Period (Day of the Year 1991)	Mass Flux	POM Flux	$CaCO_3$ Flux	Lithogenic Flux
Eumeli 1000 m	44-184	339±23	93±10	160±17	54±7
BOFS 1140 m	48-181	248±14	60±5	105±10	46±5
BOFS 1140 m / Eumeli 1000 m		73%±6	65%±9	65%±9	84%±14
Eumeli 2500 m	44-134	332±21	80±8	173±20	63±8
BOFS 2190 m	48-132	205±9	44±3	84±7	53±5
BOFS 2190 m / Eumeli 2500 m		62%±5	55%±7	49%±7	84%±13

Errors on analyses are stated in Figure 2. Fluxes in units mg m^{-2} d^{-1}.

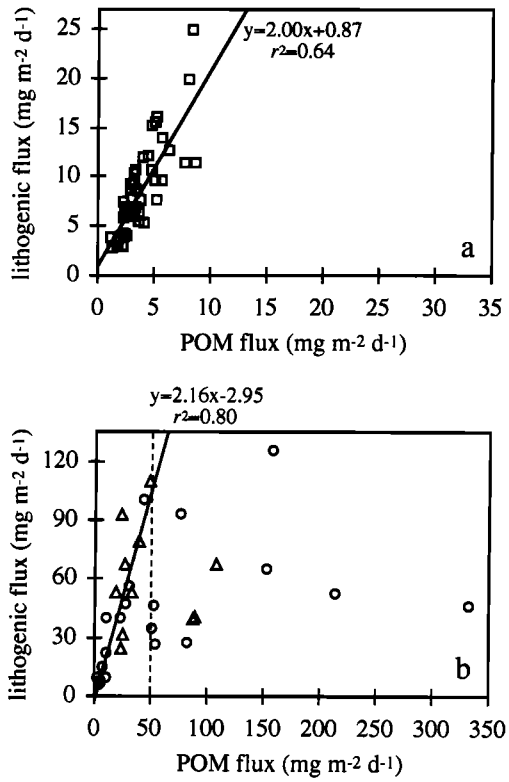

Figure 6. Lithogenic versus POM flux at (a) the oligotrophic (1000 m depth) and (b) the mesotrophic (1000 m (circles) and 1140 m (triangles) depths) sites.

tion of the estimated primary production at the mesotrophic site (~4.6% at 1000 m depth) compared to the oligotrophic site (0.6%), as expected from the trophic status of the two provinces [*Eppley*, 1989; *Wollast*, 1998]. Biogenic fluxes in the mesotrophic region are the highest recorded in the open northeast Atlantic Ocean [*Jickells et al.*, 1996], while those at the oligotrophic site are typical of more oligotrophic open–ocean records [e.g., *Deuser*, 1986; *Karl et al.*, 1996].

5.2. Particle Flux Trends With Depth

Multidepth sampling of particle flux has the potential to provide information on the characteristics of particulate matter transfer down through the water column. Averaged fluxes of the more refractory components (the lithogenic fraction in particular) show relatively good conservation with depth at the three sites. However, average mass and lithogenic fluxes do increase by about 15 and 30%, respectively, between 1000 and 2500 m at the Eumeli mesotrophic site, and to a lesser extent at the Eumeli oligotrophic site (<5% and ~15%), while lithogenic flux remains steady with depth at the BOFS site. Apparent increases with depth could be due to (1) differences in the particle source regions " feeding " the traps from surface waters, (2) lateral advection of resuspended particles, (3) hydrodynamic artefacts, or (4) midwater packaging, none of the above being mutually exclusive.

Conservation of mass flux with depth is highest when mass flux is high, which is apparent at the Eumeli mesotrophic site during the main flux events in particular (Figure 3a). When mass flux is low, such as in the oligotrophic region or at the end of the deployment at the Eumeli mesotrophic site, conservation can be poor. These differences probably reflect differences in settling rates, which seem to be higher at high mass fluxes, and the consequent differences in the " statistical funnel " dimensions within which traps are supposed to collect settling particles [*Deuser et al.*, 1988; *Deuser et al.*, 1990]. Indeed, very high settling rates (≥500 m d^{-1}) at the Eumeli mesotrophic site during the main flux events compare to the moderate settling rates of ~150 m d^{-1} at the oligotrophic site (the later falling within the typical open–ocean range [*Newton et al.*, 1994; *Honjo*, 1996, and references therein]). Such fast–settling particles at the mesotrophic site, associated with large mass fluxes (up to ~800 mg m^{-2} d^{-1}), could result from high particle concentrations in surface waters propitious for intense aggregation processes [e.g. *Alldredge and Gotschalk*, 1988]. Thus, despite the more turbulent flow conditions in the mesotrophic region (compare Appendix), statistical funnels are smaller during the main flux events than at the oligotrophic site (Table 3), indicating a more vertical trajectory for the collected particles which could explain the better flux conservation with depth. When settling rate is lower (here, flux smaller), statistical funnels are larger, and traps at different depths are more likely to collect particles originating from different surface waters, therefore reflecting the heterogeneity of particle sources at the ocean surface [*van Camp et al.*, 1991; *Gabric et al.*, 1993; *Dadou et al.*, 1996]. Thus the time series

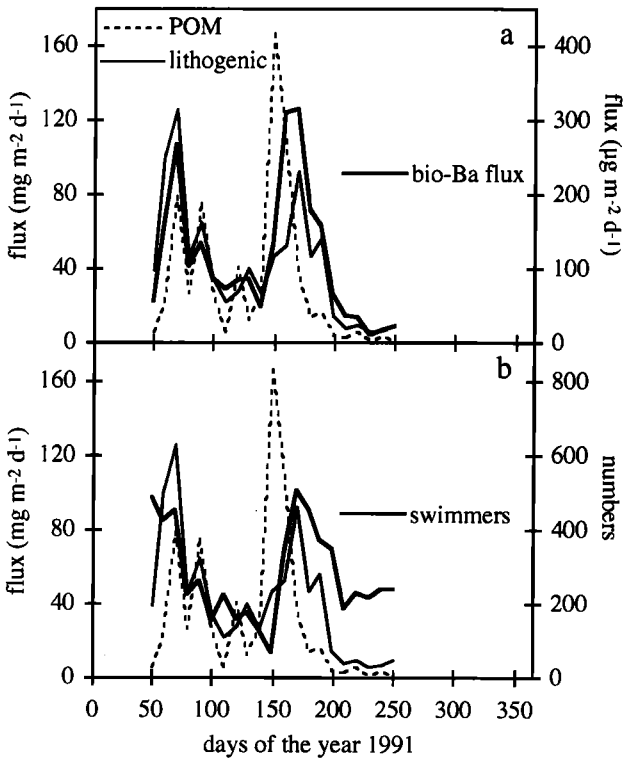

Figure 7. Lithogenic and POM fluxes (left-hand axes) plotted together with (a) biogenic barium flux and (b) number of swimmers in the collection cup (right-hand axes) at the Eumeli mesotrophic site (1000 m trap).

Table 3. Estimates of Statistical Funnel Dimensions at the Three Trap Sites

Trap	$R_{0.95}$, km
Eumeli Oligotrophic Site	
1000 m	115
2500 m	200
Eumeli Mesotrophic Site	
1000 m	57
2500 m	95
BOFS Mesotrophic Site	
1140 m	62
2190 m	88
3190 m	107

Radius ($R_{0.95}$) of the catchment areas of the traps (intersection of the statistical funnels with the ocean surface), corresponding to a 95% probability threshold of the collected particles, are presented (calculation details are given in Apendix).

seem to demonstrate physically reasonable relationships between mass flux, settling rate, and flux conservation with depth, apparently consistent with theoretical expectations [see *Fowler and Knauer*, 1986; *Siegel et al.*, 1990; *Siegel and Deuser*, 1997].

At the Eumeli mesotrophic site, where the largest average mass and lithogenic flux increases are observed with depth, most of the difference is gained toward the end of the deployment, when mass flux is relatively low (Figure 3a). Following the preceding arguments, the increase in mass flux with depth during this period, which is small in comparison to the amplitude of the flux variations at that site, could largely be due to different surface water origins of the particles. At that time, relatively higher (~fivefold) lithogenic flux at 2500 m compared to 1000 m could alternatively indicate a lateral advection of resuspended particles coming from a region nearer the coast. However, a few nephelometric profiles determined at both Eumeli sites in February 1991 have shown no nepheloid layer in the intermediate or deep water column [*Vangriesheim et al.*, 1993]. Moreover, a significant increase of $CaCO_3$ and POM fluxes between the two depths (~fivefold and twofold, respectively) is also observed, resulting in only a moderate change of average composition with depth. Thus, even if a midwater nepheloid source (likely to be of markedly different composition) cannot be ruled out, supply of material from particle–rich surface waters further from the mooring location would seem to be the most likely explanation for such an occasional particle flux increase with depth. The increase would thus reflect the heterogeneity of the surface water particle sources which, owing to the main current direction, may simply be a westward decreasing gradient of the settling particle sources [*Siegel et al.*, 1990].

However, hydrodynamic artefacts could also play a role; a possible mild under–collection at 1000 m due to current speeds occasionally close to the presumed critical threshold of 15 cm s^{-1} (see Results) could also explain some of the observed flux differences between depths [*Gardner*, 1980; *Baker et al.*, 1988; *Gust et al.*, 1992, 1994]. The fact that discrepancies occur preferentially at low mass flux could be explained by a bias that depends on the settling rate and therefore on the approach angle of sinking particles to a trap [*Siegel and Deuser*, 1997]. *Bacon* [1996] reports, from radionuclide measurements, that traps show a significant tendency toward undertrapping at depths shallower than 1200 m. Results obtained at the Eumeli sites are consistent with the hydrodynamic bias hypothesis for explaining why a slight increase of mass flux with depth is such a common feature in the intermediate water column [*Walsh et al.*, 1988]. But this hypothesis is not thought to be able to explain a difference such as the one recorded at the end of the Eumeli mesotrophic deployment, especially as current speeds remained below the threshold during this period. Finally, biological packaging in the intermediate water column could also explain an increase of particle flux with depth [*Walsh et al.*, 1988], but there is little support for this hypothesis here, as such a phenomenon might be expected to also occur at the BOFS site, which does not appear to be the case.

Differences in particle source regions, more likely to occur at low settling rates, together with a possible additional slight undertrapping at 1000 m depth, are therefore the most probable explanations for the apparent tendency of particle flux to sometimes increase with depth at the Eumeli sites. Moreover, the fact that at all three sites magnitude and temporal variability of the particulate flux obtained at different depths are consistent with each other, showing a good " vertical " transfer of the flux signal, clearly indicates a dominant surface origin for the particulate matter collected in all traps.

5.3. Coupling/Decoupling of Biogenic and Lithogenic Fluxes

The absence of a marked seasonal mass flux variability at the oligotrophic site (Figure 2a) is consistent with the nonappearance of a deep winter mixed layer at this latitude [*Levitus*, 1982] and thus little seasonality in primary productivity [*Morel et al.*, 1996]. The particle flux variability that there is may result from the variable influence of the remote coastal upwelling as suggested by *Berthon* [1992]; either from the upwelling activity itself, and/or from the intensity of the currents advecting pigment–rich water masses from the upwelling area. Faster flux fluctuations, on a timescale of 1-2 months, could be due to periodic westward currents associated with the Cape Verde Frontal Zone oscillations, or be related to the reproductive cycles of some planktonic organisms as discussed by *Khripounoff et al.* [1998]. Alternatively, meandering structures leading to eddy upwellings within the NEC could lead to episodic enhanced productivity production [*Dadou et al.*, 1996].

Mass fluxes in the mesotrophic region also show little by way of a marked seasonal signal (Figures 3a and 5a). Large changes in flux occur all year round and are likely to reflect mainly the fluctuating effect of the upwelling [*van Camp et al.*, 1991; *Berthon*, 1992; *Gabric et al.*, 1993]. Such an influence is supported by analyses of phytoplankton community structure, carried out in September-October 1991 and April-May 1992, which indicate a declining bloom that has evolved from an autotrophic community developed under eutrophic conditions and advected to the mesotrophic site [*Claustre*, 1994].

While lithogenic and POM fluxes at the oligotrophic site are linearly correlated over the entire flux range, those in the mesotrophic are not (section 4.4, Figure 7). In the mesotrophic region, a strong decoupling of the major components of

the particle flux occurs; lithogenic flux peaks in winter, while very large POM fluxes are recorded in spring, when the highest primary productivity is expected [*Morel et al.*, 1996]. The linear relationship between lithogenic and POM fluxes generally observed in regions subject to aeolian dust inputs has been interpreted as biological control of the removal of lithogenic particles from surface waters [*Deuser et al.*, 1983]. This relationship implies that in these regions (1) lithogenic flux is a good tracer of POM flux, and vice versa, and (2) lithogenic flux is likely to be quantitatively limited by the export of biogenic material, at an average Al/POC ratio given by the slope of the linear relationship. Consequently, the surprising break in the proportional relationship in the mesotrophic region, associated with lower and more variable Al/POC at higher POM fluxes (section 4.4), may indicate that the biogenic particle flux exceeds the lithogenic particle stock (i.e., there is insufficient lithogenic material in the water column to meet the lithogenic transport " capacity " of the POM). It can therefore be argued that a more efficient transport of lithogenic material down through the water column occurs in the mesotrophic region than at the oligotrophic site. The relative particulate aluminium residence time estimates for the two sites (section 4.5) are in agreement with a more efficient transport in the mesotrophic region.

Furthermore, on short timescales, the timing of lithogenic and POM flux peaks does not systematically coincide. For the second large flux event in the Eumeli mesotrophic region, lithogenic flux peaks ~20 days after the POM flux, yet biogenic barium and lithogenic fluxes correlate well (Figure 7). Biogenic barium (calculated as total Ba - (Al X 0.0075) [*Dymond et al.*, 1992, and references therein] is thought to be formed in surface and hemipelagic waters within degrading organic particles [*Chow and Goldberg*, 1960; *Dehairs et al.*, 1980; *Bishop*, 1988] or by active biological processes [*Bertram and Cowen*, 1997]. As the lithogenic and barium particulates have different sources, the covariation of their fluxes suggests that they are transported by common processes. The export of particulate matter occurs mainly as fecal pellets [*Dunbar and Berger*, 1981; *Krishnaswami et al.*, 1985; *Pilskaln and Honjo*, 1987], and large aggregates (" marine snow " [*Asper*, 1987; *Alldredge and Gotschalk*, 1988; *Alldredge and Silver*, 1988]). Lithogenic particles are thought to be transported mainly as fecal pellets [*Fowler and Knauer*, 1986; *Buat-Ménard et al.*, 1989; *Davies and Buat-Ménard*, 1990]. If so, the lag between POM and lithogenic flux peaks during the second flux event could be explained by a classical sequence [*Honjo*, 1996]: the fallout of a (aggregated) phytoplankton bloom could give rise to the large POM flux (with the presence of diatoms as suggested by the opal flux peaks; Figure 3b) followed by grazing by zooplankton which could incidentally package and export lithogenic and biogenic-barium particles as fecal pellets. The number of swimmers (mostly copepods; N. Leblond, personal communication, 1997) collected in the traps peaks with lithogenic and biogenic barium fluxes (Figure 7); if we assume that these swimmer numbers are roughly proportional to those of zooplankton above the trap (in surface and hemipelagic waters where most grazing and packaging should arise), the hypothesis of the dominance of fecal pellets in the transfer of lithogenic particles is supported. The drastic change in the lithogenic/POM flux relationship at that site could thus also derive partly from changes in the ecosystem during the evolution of blooms which would lead to changes in the nature and source of the exported POM. This hypothesis would also explain why linear relationships between lithogenic and POM fluxes do not all show the same slope [e.g. *Deuser et al.*, 1983; *Jickells et al.*, 1990; *Neuer et al.*, 1997]; slope would be dependent on the nature of the settling biogenic matter, which can vary widely from one area to another [e.g., *Honjo*, 1996].

5.4. Mesoscale Variability in the Mesotrophic Region

The mesoscale variability of particle flux, which is mainly due to variability in the biogenic fluxes (section 4.3), probably reflects the spatial heterogeneity of biogenic particle production and export in the surface waters. That such heterogeneity can occur in this region is clearly observed on satellite images that show the meandering structures of the biomass–rich filaments, extending from shelf regions, which can reflect sharp gradients in primary productivity over tens of kilometers [*Berthon*, 1992]. Considering the distance between the two moorings (~100 km) and the size of the statistical collec-

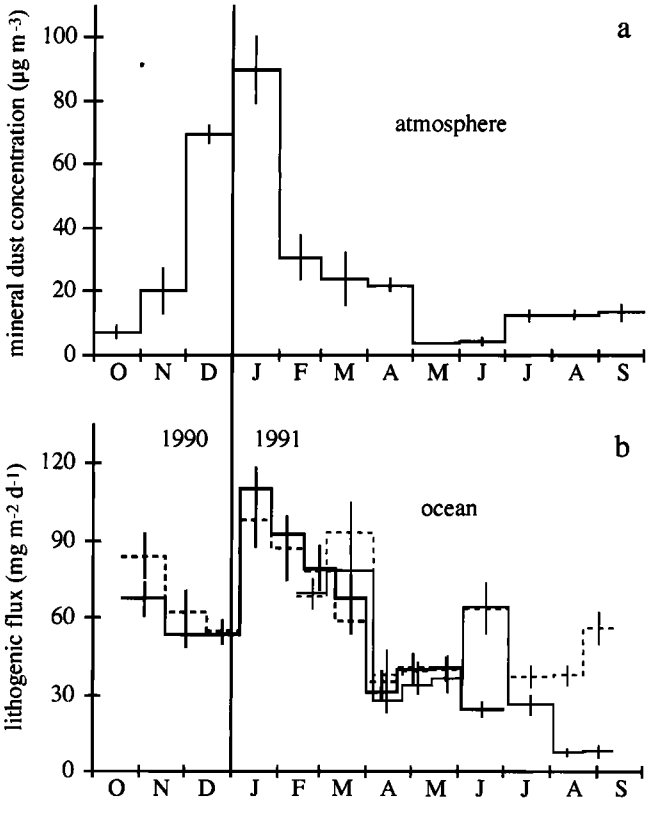

Figure 8. (a) Average monthly mean of the atmospheric mineral dust concentration at Sal for the period 1992-1994 [from *Chiapello et al.*, 1995; *Chiapello*, 1996]. (b) Lithogenic fluxes in the mesotrophic region. Errors on analyses are stated in Figures 2 and 3. Plain thick and thin lines, BOFS 1140 m and Eumeli 1000 m depth traps, respectively; dotted thick and thin lines, BOFS 2190 m and Eumeli 2500 m depth traps, respectively.

tion areas (Table 3), Eumeli and BOFS traps, which sample a small surface of the ocean at a given time (not larger than a few hundred meters [*Siegel and Deuser*, 1997]), are very likely to record in some way such a spatial heterogeneity of the particle source. The two main biogenic flux events recorded (Figure 5) could therefore correspond to export from such filaments, but an export that might not have " fed " to the same extent into the Eumeli and BOFS traps, leading to the distinct differences observed in the magnitude and timing of particle flux at the two sites. The relative lack of mesoscale variability, both in terms of magnitude and timing, for lithogenic fluxes (section 4.3), is consistent with the expectation that atmospheric inputs of mineral dust are similar over the spatial scale covering both sites (taking into account the distance to the dust source areas (up to several thousands kilometers [*Chiapello*, 1996]) and the size of the dust clouds (order of magnitude of 10^6 km^2 [*Moulin et al.*, 1997a])). These observed patterns of mesoscale variability support the hypothesis that biological activity in this region, despite its apparent spatial and temporal variability, is high enough most of the time to ensure the rapid and efficient transfer of the mineral dust inputs to the deep ocean.

5.5. Atmospheric Dust Inputs

The lithogenic flux time series in the water column in the mesotrophic region (1990-1991) and the average (1992-1994) annual cycle in atmospheric dust concentration at ground level over the nearby Cape Verde Islands [*Chiapello et al.*, 1995; *Chiapello*, 1996] show a similar temporal pattern (Figure 8); 1990-1991 atmospheric dust concentrations were not measured. The highest atmospheric loading occurs in December and January, a few weeks, at most, before the lithogenic flux peak in the water column at ~1 km depth (Figure 4b). One can assume that atmospheric dust deposition varies with the concentration at ground level, because no significant rainfall that could potentially scavenge and deposit dust from above the trade wind layer occurs (B. Chatenet, personal communication, 1997). Therefore, even if large variations in the export of biogenic material (in spring, for instance) are likely to drive part of the lithogenic flux variability in the water column (Figure 3b), the latter mainly reflects the seasonal variability of the atmospheric dust inputs. These results again support the rapid and efficient mechanism of downward transport of dust in the water column of the mesotrophic region.

At the oligotrophic site, the seasonal variability of dust concentration in the lower atmosphere was similar to that observed at Sal, although less marked [*Bory*, 1997]. While it can be argued that rainfall can play a more significant role in controlling dust deposition than in the mesotrophic region (W. Guelle, personal communication, 1997), it has been shown not to be the case during the sampling period [*Bory*, 1997].

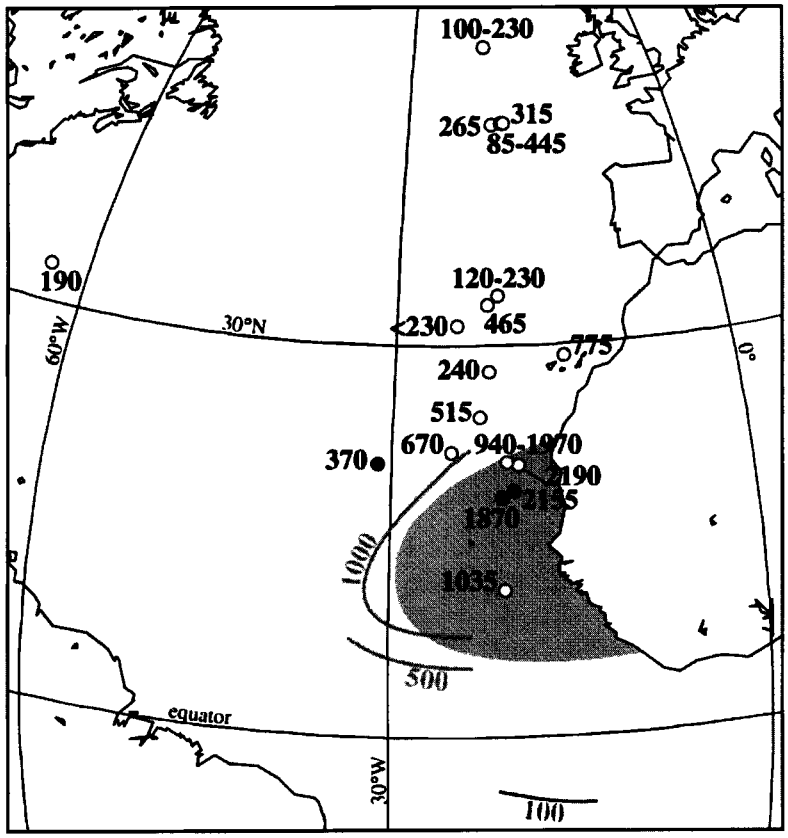

Figure 9. Compilation of lithogenic fluxes, expressed in mg cm^{-2} kyr^{-1}, in the water column (solid circle, this study; open circles, other trap locations) and surface sediments (contours, *Rea* [1994]) in the North Atlantic. Values have been rounded to the nearest 5 mg cm^{-2} kyr^{-1}. Full references are given in Table 4. Rough atmospheric dust plume contour is indicated through gray shading marking out ~75% of the moderate–to–heavy dust outbreaks (i.e., dust optical thickness ≥0.30) for 1989-1990 [*Swap et al.*, 1996]. Geographical map was obtained from M. Weinelt (<http://www.aquarius.geomar.de/omc/>, 1999).

Dust deposition should therefore vary with atmospheric dust concentration, yet the lithogenic flux in the water column does not reflect the atmospheric signal in this way. Instead, the lithogenic flux variations in the water column mimic those of the export of the biogenic components (Figure 2b). These results are in agreement with the slower, and apparently limited, transfer of lithogenic particles in the water column in the oligotrophic region. A recent study in the oligotrophic Sargasso Sea yielded similar findings [*Jickells et al.*, 1998].

5.6. Regional Features of Lithogenic Fluxes in the Water Column

Averaged water column lithogenic fluxes recorded in this study, together with other data collected from the North Atlantic Ocean during the last decade, are presented in Figure 9 and Table 4. Most of the fluxes beyond this study have been calculated indirectly (mass flux minus biogenic flux; see Table 4), therefore increasing the uncertainties on the flux estimates. Moreover, results presented were obtained at different time periods over different sampling duration (7 to 32 months), and interannual variability is probable [*Fischer et al.*, 1996]. The spatial patterns of the averaged lithogenic fluxes nevertheless appear to be consistent with the lithogenic accumulation rates in the bottom sediments over the last hundreds/thousands of years (Figure 9). Both data sets present a tongue pattern oriented west to southwest with higher values at about 15°-20°N nearshore, decreasing with the distance from the coast as well as northward and southward.

The same spatial pattern is also shown by the time-averaged atmospheric dust concentrations obtained from remote-sensing data (Figure 9) [*Swap et al.*, 1996; *Husar et al.*, 1997; *Moulin et al.*, 1997a, b], the qualitative dust falls records on ships [*Semmelhack*, 1934; *Kuenen*, 1950; *Schütz*, 1980], and the mean dust deposition flux estimates obtained from near-surface dust concentration data [*Duce et al.*, 1991]. Although atmosphere-ocean and water column dust fluxes are roughly consistent when comparing time mean values over large spatial areas, surface water circulation and atmospheric dust deposition in the study regions during sediment trap de-

Table 4. Average Lithogenic Contents of the Particulate Matter and Lithogenic Fluxes in the Deep North Atlantic Water Column

Site	Deployment Time	Lithogenic Content %	Lithogenic Flux mg m^{-2} d^{-1}	Source
54°35'N, 21°09'W	June 10, 1992 to May 12, 1993	7	2.8	*Kuss and Kremling* [1999]
	Sept. 27, 1993 to May 24, 1994	9	5.0	*Kuss and Kremling* [1999]
47°50'N, 19°30'W	April 18, 1989 to Sept. 16, 1990	12	7.3	*Jickells et al.* [1996]
47°49'N, 19°45'W	March 27, 1992 to Sept. 18, 1992	13	12.2	*Kuss and Kremling* [1999]
	June 10, 1992 to May 26, 1993	6-13	2.3-4.9	*Kuss and Kremling* [1999]
	Sept. 20, 1993 to June 16, 1994	8	5.1	*Kuss and Kremling* [1999]
47°43'N, 20°52'W	April 3, 1989 to April 16, 1990	12	8.6	*Honjo and Manganini* [1993]
33°49'N, 21°01'W	April 3, 1989 to April 16, 1990	22	12.8	*Honjo and Manganini* [1993]
33°09'N, 21°59'W	Sept. 20, 1993 to Sept. 1, 1994	6-13	3.2-6.3	*Kuss and Kremling* [1999]
32°05'N, 64°15'W	1981 - 1991	20	5.2	*Jickells et al.* [1998]
31°33'N, 24°40'W	Dec., 1985 to Nov., 1986	<19	<6.3	*Lampitt* [1992]
29°08'N, 15°26'W	1992 - 1994	-	21.2	*Ratmeyer et al.* [1999]
28°00'N, 21°59'W	Oct. 7, 1990 to July 28, 1991	24	6.6	*Jickells et al.* [1996]
24°33'N, 22°50'W	Oct. 14, 1990 to Sept. 27, 1991	35	14.3	*Jickells et al.* [1996]
21°56'N, 25°14'W	Dec. 1, 1986 to April 30, 1987	34	18.3	*Kremling and Streu* [1993]
21°09'N, 20°41'W	March 15, 1989 to March 24, 1990	38	54.0	*Fischer et al.* [1996]
	April 29, 1990 to April 8, 1991	39	53.2	*Fischer et al.* [1996]
	May 3, 1991 to Nov. 19, 1991	37	25.8	*Fischer et al.* [1996]
21°03'N, 31°10'W	March 5, 1991 to May 6, 1992	28	10.2	this study
20°55'N, 19°45'W	March 22, 1988 to March 8, 1989	41	60.0	*Fischer et al.* [1996]
19°00'N, 20°10'W	Oct. 21, 1990 to June 30, 1991	23	59.0	this study
18°30'N, 21°05'W	Feb. 13, 1991 to Sept. 13, 1991	20	51.3	this study
11°29'N, 21°02'W	1993 - 1994	-	28.4	*Ratmeyer et al.* [1999]

Updated from *Jickells et al.* [1996]. All values have been obtained indirectly (mass flux minus biogenic fluxes (POM, $CaCO_3$ and opal)), except for *Kremling and Streu* [1993], *Kuss and Kremling* [1999], and this study where lithogenic matter is estimated from aluminium measurements considering a concentration of 8.4% Al [*Turekian and Wedepohl*, 1961]. Opal was not measured by *Lampitt* [1992].

ployments would have to be estimated if the quantitative transfer of dust from the atmosphere to the deep ocean is to be assessed. The development of dust transport models [*Guelle et al.*, 1998; *Schulz et al.*, 1998] should enable such evaluations.

6. Summary and Conclusions

1. The high percentage (~20-30% on average) of lithogenic matter in the trap material collected at all three sites shows the regional significance of atmospheric dust inputs. The magnitude of both lithogenic and biogenic fluxes decreases ~5-6 and ~8-9 fold, respectively, between the mesotrophic and oligotrophic sites, from near the African margin (i.e., the high–productivity coastal upwelling zone and near the dust source areas) to the remote open ocean. The lithogenic fluxes do not vary significantly with depth in either region, indicating that no major lateral advection of terrigenous material occurs in the intermediate water column. High–flux episodes in the mesotrophic region are associated with high settling rates (≥500 m d^{-1}), compared to the oligotrophic region where settling rates of ~150 m d^{-1}, more typical of the open ocean, are recorded.

2. Differences in the trophic status of the two sites seem to give rise to differences in the characteristics of the downward transport of the lithogenic material. At the oligotrophic site the relatively low and slow export of biogenic matter apparently limits and delays the downward transport of lithogenic particles delivered to surface waters from the atmosphere. In contrast, the higher biological activity at the mesotrophic sites seems to provide persistent conditions for an efficient and faster downward transport of the deposited lithogenic particles (possibly largely in fecal material), and the temporal variability of lithogenic flux largely reflects that of the atmospheric dust inputs. Thus whether the temporal variability of the exported lithogenic flux in the water column follows that of the atmospheric signal appears to depend on the trophic status of the oceanic province.

3. Results obtained at the mesotrophic sites show that the oft–observed linear relationship between lithogenic and POM fluxes breaks down at high POM fluxes. At these sites, the same nonlinear relationship is observed between biogenic barium and POM, as well as between ^{210}Pb and POM [*Legeleux et al.*, 1996] fluxes. Such nonlinear relationships at high particle fluxes have been previously observed for ^{210}Pb and ^{230}Th in the North Atlantic [*Colley et al.*, 1995]. These results add weight to the idea that linear relationships between some candidate proxies and POM fluxes cannot be assumed under conditions of high POM export, in this case, for about one quarter of the annual cycle, during which about 70% of the total POM flux occurs.

4. The high mesoscale variability of biogenic, but not lithogenic, fluxes in the water column at the mesotrophic site extends the evidence for such variability in high–production areas beyond the temperate northeast Atlantic Ocean [*Newton et al.*, 1994]. The relevance of mesoscale studies (or of long time series [*Deuser*, 1996]) for regional carbon export budget estimates in the ocean is thus underscored.

Appendix

Using a Lagrangian analysis of the sinking particles through a random mesoscale eddy field, *Siegel et al.* [1990] have proposed a theoretical estimate of the catchment area of a trap which depends on the sinking speed of the particles and on the velocity field above the trap. In this study, the catchment area is estimated by the standard deviation of the statistical probability density function of the particles collected by the trap (normal distribution) in the radial direction, Lx (km), calculated as $Lx=2\{KE(\tau T-\tau^2(1-\exp(-T/\tau)))\}^{1/2}$, where KE ($cm^2\ s^{-2}$) is the vertically averaged eddy kinetic energy over the trap, τ (seconds) is the Lagrangian decorrelation timescale (which quantifies the decorrelation time scale of a fluid parcel's horizontal velocity with itself), and T (seconds) is the time required for the particle to sink from the sea surface to the trap. The cumulative fraction of the total number of particles found within a radial distance R of the center of the collection distribution is then equal to $P(x\leq R)=1-\exp(-R^2/(2Lx^2))$. The 95% collection probability threshold corresponds to a distance of ~$2.45Lx$ from the center. Variable τ and the eddy kinetic energy have been calculated at each Eumeli site from the current data at 250, 1000, and 2500 m depth (A. Vangriesheim, personal communication, 1997); τ has been estimated to be ~15 days at both mesotrophic and oligotrophic sites, and eddy kinetic energies have been estimated to be 99/16/4 and 36/16/5 $cm^2\ s^{-2}$ at 250/1000/2500 m at the mesotrophic and oligotrophic sites, respectively. KE values over the traps (72/33 and 29/17 $cm^2\ s^{-2}$ for the 1000/2500 m Eumeli mesotrophic and oligotrophic traps, and 65/37/27 for the 1140/2190/3190 m BOFS traps) were obtained using an exponential equation to represent the eddy kinetic energy profile as suggested by *Siegel and Deuser* [1997], which was integrated over the corresponding water column depths (for example, 0 to 1000 m for the 1000 m depth trap). Mean sinking times have been calculated by dividing depth by the estimated settling rates at the mesotrophic (500 m d^{-1}) and oligotrophic (150 m d^{-1}) sites. For each trap, $R_{0.95}$, the catchment areas of the traps corresponding to a 95% probability threshold of the collected particles, was then calculated using these parameters and the above equations.

Acknowledgements. We thank N. Leblond (Eumeli) and C. Boutle (BOFS) for swimmer picking and for providing mass flux data. We thank A. Vangriesheim, H. Etcheber, and C. Rabouille from the Eumeli program, for providing current, POC, and opal data, respectively. From the BOFS program, we thank P. King for providing POC and opal data. We also thank I. Chiapello for giving us access to her atmospheric dust concentration data, and T. Jickells and his team for providing ICP-AES facilities. A. Bory thanks the Ministère de l'Education Nationale, de la Recherche et de la Technologie that awarded his Ph.D. grant. P. Newton thanks Oxford Brookes University for a Visiting Research Fellowship. The manuscript benefited from the helpful comments of two anonymous reviewers. LSCE contribution 302.

References

Alldredge, A.L., and C. Gotschalk, In situ settling behavior of marine snow, *Limnol. Oceanogr.*, *33*, 339-351, 1988.

Alldredge, A.L., and M.W. Silver, Characteristics, dynamics and significance of marine snow, *Prog. Oceanogr.*, *20*, 41-82, 1988.

Alpert, P., Y.J. Kaufman, Y. Shay-El, D. Tanré, A. da Silva, S. Schubert, and J.H. Joseph, Quantification of dust–forced heating of the lower troposphere, *Nature*, *395*, 367-370, 1998.

Asper, V.L., Measuring the flux and sinking speed of marine snow aggregates, *Deep Sea Res.*, *34*, 1-17, 1987.

Bacon, M.P., Evaluation of sediment traps with naturally occurring radionuclides, in *Particle Flux in the Ocean*, SCOPE report vol. 57, edited by V. Ittekkot et al., pp. 85-90, John Wiley, New York, 1996.

Baker, E.T., H.B. Milburn, and D.A. Tennant, Field assessment of sediment trap efficiency under varying flow conditions, *J. Mar. Res., 46*, 573-592, 1988.

Ballouey, J., Etude des flux de silice biogénique, in *Rapport de stage de fin d'étude*, Cent. des Faibles Radioactiv., Gif-sur-Yvette, France, 1994.

Behrenfeld, M.J., A.J. Bale, Z.S. Kolber, J. Aiken, and P.G. Falkowski, Confirmation of iron limitation of phytoplankton photosynthesis in the equatorial Pacific Ocean, *Nature, 383*, 508-511, 1996.

Berthon, J.F., Evaluation de la biomasse phytoplanctonique et de la production primaire associée à partir des données satellitaires ("couleur de l'océan"): Application à la zone tropicale au large de la Mauritanie (utilisation de l'imagerie du CZCS), Thèse de doctorat, Univ. Paris 6 Pierre et Marie Curie, Paris, 1992.

Bertram, M.A., and J.P. Cowen, Morphological and compositional evidence for biotic precipitation of marine barite, *J. Mar. Res., 55*, 577-593, 1997.

Bishop, J.K., The barite–opal–organic carbon association in oceanic particulate matter, *Nature, 332*, 341-343, 1988.

Bishop, J.K.B., Regional extremes in particulate matter composition and flux: effects on the chemistry of the ocean interior, in *Productivity of the Ocean: Present and Past*, edited by W. H. Berger, V. S. Smetacek, and G. Wefer, pp. 117-137, John Wiley, New York, 1989.

Bory, A., Etude des flux de matériel terrigène dans la colonne d'eau de l'Atlantique subtropical nord-est: Relations avec les apports atmosphériques, Thèse de doctorat, 265 pp., Univ. Paris 7 Denis Diderot, Paris, 1997.

Bournot, C., A. Vangriesheim, and A. Vigot, Rapport de données de courant des mouillages de pièges (250 - 1000 - 2500 m) - Campagnes Eumeli 2 à 5, Joint Global Ocean Flux Study-France, Plouzané, 1995.

Bowen, H.J.M., *Trace Elements in Biochemistry*, Academic, San Diego, Calif., 1966.

Buat-Ménard, P., J.E. Davies, E. Remoudaki, J.-C. Miquel, G. Bergametti, C.E. Lambert, U. Ezat, C. Quétel, J. La Rosa, and S.W. Fowler, Non–steady–state biological removal of the atmospheric particles from Mediterranean surface waters, *Nature, 340*, 131-133, 1989.

Chiapello, I., Les aérosols atmosphériques au-dessus de l'Atlantique nord tropical: Approche physico-chimique et météorologique: Evaluation de la contribution des différentes espèces à l'épaisseur optique en aérosol, Thèse de doctorat, 250 pp., Univ. Paris 7 Denis Diderot, Paris, 1996.

Chiapello, I., G. Bergametti, L. Gomes, and B. Chatenet, An additional low layer transport of Sahelian and Saharan dust over the northeastern tropical Atlantic, *Geophys. Res. Lett., 22*, 3191-3194, 1995.

Chow, T.J., and E.D. Goldberg, On the marine geochemistry of barium, *Geochim. Cosmochim. Acta, 20*, 192-198, 1960.

Claustre, H., The trophic status of various oceanic provinces as revealed by phytoplankton pigment signatures, *Limnol. Oceanogr., 39*, 1206-1210, 1994.

Coale, K.H., S.E. Fitzwater, R.M. Gordon, K.S. Johnson, and R.T. Barber, Control of community growth and export production by upwelled iron in the equatorial Pacific Ocean, *Nature, 379*, 621-624, 1996a.

Coale, K.H., et al., A massive phytoplankton bloom induced by an ecosystem-scale iron fertilization experiment in the equatorial Pacific Ocean, *Nature, 383*, 495-501, 1996b.

Colley, S., J. Thomson, and P. Newton, Detailed ^{230}Th, ^{232}Th and ^{210}Pb fluxes recorded by the 1989/90 BOFS sediment trap time-series at 48°N, 20°W, *Deep Sea Res. Part I, 42*, 833-848, 1995.

Dadou, I., V. Garçon, V. Andersen, G.R. Flierl, and C.S. Davis, Impact of the North Equatorial Current meandering on a pelagic ecosystem: A modeling approach, *J. Mar. Res., 54*, 311-342, 1996.

Darwin, C., An account of the fine dust which falls on vessels in the Atlantic Ocean, *Q. J. Geol. Soc. London, 2*, 26-30, 1846.

Davies, J.E., and P. Buat-Ménard, Impact of atmospheric deposition on particulate manganese and aluminium distribution in northwestern Mediterranean surface water, *Palaeogeogr. Palaeoclimatol. Palaeoecol., 89*, 35-45, 1990.

Dehairs, F., R. Chesselet, and J. Jedwab, Discrete suspended particles of barite and the barium cycle in the open ocean, *Earth Planet. Sci. Lett., 49*, 528-550, 1980.

Deuser, W.G., Seasonal and interannual variations in deep-water particle fluxes in the Sargasso Sea and their relationship to surface hydrography, *Deep Sea Res., 33*, 225-246, 1986.

Deuser, W.G., Temporal variability of particle flux in the deep Sargasso Sea, in *Particle Flux in the Ocean*, SCOPE report vol. 57, edited by V. Ittekkot et al. , pp. 185-198, John Wiley, New York, 1996.

Deuser, W.G., P.G. Brewer, T.D. Jickells, and R.F. Commeau, Biological control of the removal of abiogenic particles from the surface ocean, *Science, 219*, 388-391, 1983.

Deuser, W.G., F.E. Muller-Karger, and C. Hemleben, Temporal variations of particle fluxes in the deep subtropical and tropical North Atlantic: Eulerian versus Lagrangian effects, *J. Geophys. Res., 93*, 6857-6862, 1988.

Deuser, W.G., F.E. Muller-Karger, R.H. Evans, O.B. Brown, W.E. Esaias, and G.C. Feldman, Surface–ocean color and deep–ocean carbon flux: How close a connection?, *Deep Sea Res., 37*, 1331-1343, 1990.

Duce, R., et al., The atmospherical input of trace species to the world ocean, *Global Biogeochem. Cycles, 5*, 193-259, 1991.

Dunbar, R.B., and W.H. Berger, Fecal pellet flux to modern bottom sediment of Santa Barbara Basin (California) based on sediment trapping, *Geol. Soc. Am. Bull., 92*, 212-218, 1981.

Dymond, J., E. Suess, and L. Mitch, Barium in deep–sea sediment: A geochemical proxy for paleoproductivity, *Paleoceanography, 7*, 163-181, 1992.

Ehrenberg, C.G., Erläuterungen eines neuen wirklichen Passat–staubes aus dem atlantischen Dunkelmeere vom 29 Oct. 1861, in *Monatsber. Kg. Preuss. Akad. Wiss.*, pp. 202-224, Berlin, 1862.

Eppley, R.W., New production: History, methods, problems, in *Productivity of the Ocean, Present and Past*, edited by W. H. Berger, V. S. Smetacek, and G. Wefer, pp. 85-97, John Wiley, New York, 1989.

Fischer, G., B. Donner, V. Ratmeyer, R. Davenport, and G. Wefer, Distinct year–to–year particle flux variations off Cape Blanc during 1988-1991: Relation to ∂^{18}O–deduced sea–surface temperatures and trade winds, *J. Mar. Res., 54*, 73-98, 1996.

Fowler, S.W., and G.A. Knauer, Role of large particles in the transport of elements and organic compounds through the oceanic water column, *Prog. Oceanogr., 16*, 147-194, 1986.

Gabric, A.J., L. Garcia, L. van Camp, L. Nykjaer, W. Eifler, and W. Schrimpf, Offshore export of shelf production in the Cape Blanc (Mauritania) giant filament as derived from Coastal Zone Color Scanner imagery, *J. Geophys. Res., 98*, 4697-4712, 1993.

Game, P.M., Observations on a dustfall in the eastern Atlantic, February, 1962, *J. Appl. Meteorol., 34*, 355-359, 1964.

Gardner, W.D., Sediment trap dynamics and calibration: A laboratory evaluation, *J. Mar. Res., 38*, 17-39, 1980.

Greeley, R., and J.D. Iversen, Wind As a Geological Process, Cambridge Planetary Sci. Ser., Cambridge Univ. Press, New York, 1985.

Guelle, W., Y. Balkanski, M. Schulz, F. Dulac, and P. Monfray, Wet deposition in a global size-dependent aerosol transport model, 1, Comparison of a 1–year ^{210}Pb simulation with ground measurements, *J. Geophys. Res., 103*, 11,429-11,445, 1998.

Gust, G., R.H. Byrne, R.E. Bernstein, P.R. Betzer, and W. Bowles, Particle fluxes and moving fluids: Experience from synchronous trap collections in the Sargasso Sea, *Deep Sea Res., 39*, 1071-1083, 1992.

Gust, G., A.F. Michaels, R. Johnson, W.G. Deuser, and W. Bowles, Mooring line motions and sediment trap hydromechanics: In situ intercomparison of three common deployment designs, *Deep Sea Res., 41*, 831-857, 1994.

Heussner, S., C. Ratti, and J. Carbonne, The PPS 3 time-series sediment trap and the trap sample processing techniques used during the ECOMARGE experiment, *Cont. Shelf Res., 10*, 943-958, 1990.

Honjo, S., Sedimentation of materials in the Sargasso Sea at a 5367 m deep station, *J. Mar. Res., 36*, 469-492, 1978.

Honjo, S., Seasonality and interaction of biogenic and lithogenic particulate flux at the Panama basin, *Science, 218*, 883-884, 1982.

Honjo, S., Particle flux in the ocean, in *Particle Flux in the Ocean*, SCOPE report vol. 57, edited by V. Ittekkot et al., pp. 91-154, John Wiley, New York, 1996.

Honjo, S., and W.D. Doherty, Large aperture time-series sediment traps; design objectives, construction and application, *Deep Sea Res., 35*, 133-149, 1988.

Honjo, S., and S. Manganini, Annual biogenic particle fluxes to the interior of the North Atlantic Ocean; studied at 34°N 21°W and 48°N 21°W, *Deep Sea Res. Part II, 40*, 587-607, 1993.

Honjo, S., S.J. Manganini, and L.J. Poppe, Sedimentation of lithogenic particles in the deep ocean, *Mar. Geol., 50*, 199-220, 1982a.

Honjo, S., D.W. Spencer, and J.W. Farrington, Deep advective transport of lithogenic particles in Panama basin, *Science, 216*, 516-518, 1982b.

Honjo, S., D.W. Spencer, and W.D. Gardner, A sediment trap intercomparison experiment in the Panama Basin, 1979, *Deep Sea Res., 39*, 333-358, 1992.

Husar, R.B., J.M. Prospero, and L.L. Stowe, Characterization of tropospheric aerosols over the oceans with the NOAA advanced very high resolution radiometer optical thickness operational product, *J. Geophys. Res., 102*, 16,889-16,909, 1997.

Ittekkot, V., The abiotically driven biological pump in the ocean and short-term fluctuations in atmospheric CO_2 contents, *Global Planet. Change, 8*, 17-25, 1993.

Ittekkot, V., and B. Haake, The terrestrial link in the removal of organic carbon in the sea, in *Facets of Modern Biogeochemistry*, edited by V. Ittekkot et al., pp. 318-325, Springer-Verlag, New York, 1990.

Ittekkot, V., P. Schäfer, S. Honjo, and P.J. Depetris (Eds.), *Particle Flux in the Ocean*, SCOPE report vol. 57, John Wiley, New York, 1996.

Jaenicke, R., and L. Schütz, Comprehensive study of physical and chemical properties of the surface aerosols in the Cape Verde islands region, *J. Geophys. Res., 83*, 3585-3599, 1978.

Jickells, T.D., W.G. Deuser, and A.H. Knap, The sedimentation rates of trace elements in the Sargasso Sea measured by sediment trap, *Deep Sea Res., 31*, 1169-1178, 1984.

Jickells, T.D., W.G. Deuser, A. Fleer, and C. Hemleben, Variability of some elemental fluxes in the western tropical Atlantic Ocean, *Oceanol. Acta, 13*, 291-298, 1990.

Jickells, T.D., P.P. Newton, P. King, R.S. Lampitt, and C. Boutle, A comparison of sediment trap records of particle fluxes from 19° to 48°N in the northeast Atlantic and their relation to surface water productivity, *Deep Sea Res. Part I, 43*, 971-986, 1996.

Jickells, T.D., S. Dorling, W.G. Deuser, T.M. Church, R. Arimoto, and J. Prospero, Air-borne dust fluxes to a deep water sediment trap in the Sargasso Sea, *Global Biogeochem. Cycles, 12*, 311-320, 1998.

Karl, D.M., J.R. Christian, J.E. Dore, D.V. Hebel, R.M. Letelier, L.M. Tupas, and C.D. Winn, Seasonal and interannual variability in primary production and particle flux at Station ALOHA, *Deep Sea Res. Part II, 43*, 539-568, 1996.

Keil, R.G., D.B. Montluçon, F.G. Prahl, and J.I. Hedges, Sorptive preservation of labile organic matter in marine sediments, *Nature, 370*, 549-552, 1994.

Khripounoff, A., A. Vangriesheim, and P. Crassous, Vertical and temporal variations of particle fluxes in the deep tropical Atlantic, *Deep Sea Res. Part I, 45*, 193-216, 1998.

Knauer, G., and V. Asper, Sediment trap technology and sampling, in *Report of the U.S. GOFS Working Group on Sediment Trap Technology and Sampling, University of S. Mississippi, 14-18 November 1988, U.S. GOFS Plann. rep. No 10*, 94 pp., Woods Hole Oceanogr. Inst., Woods Hole, Mass., 1989.

Kremling, K., and P. Streu, Saharan dust influenced trace element fluxes in deep North Atlantic subtropical waters, *Deep Sea Res. Part I, 40*, 1155-1168, 1993.

Krishnaswami, S., M. Baskaran, S.W. Fowler, and M. Heyraud, Comparative role of salps and other zooplankton in the cycling and transport of selected elements and natural radionuclides in Mediterranean waters, *Biogeochemistry, 1*, 353-360, 1985.

Krom, M.D., N. Kress, and S. Brenner, Phosphorus limitation of primary productivity in the eastern Mediterranean Sea, *Limnol. Oceanogr., 36*, 424-432, 1991.

Kuenen, H., *Marine Geology*, John Wiley, New York, 1950.

Kuss, J., and K. Kremling, Particulate trace element fluxes in the deep northeast Atlantic Ocean, *Deep Sea Res. Part I, 46*, 149-169, 1999.

Lal, D., Comments on some aspects of particulate transport in the oceans, *Earth Planet. Sci. Lett., 49*, 520-527, 1980.

Lampitt, R.S., The contribution of deep-sea macroplankton to organic remineralisation: Results from sediment trap and zooplankton studies over Madeira Abyssal Plain, *Deep Sea Res., 39*, 221-233, 1992.

Lampitt, R.S., P.P. Newton, T.D. Jickells, J. Thomson, and P. King, Near-bottom particle flux in the abyssal Northeast Atlantic, *Deep Sea Res. Part II*, in press, 1999.

Leblond, N., E. Nicolas, and J.C. Marty, Rapport d'activité de la cellule "traitement pièges" d'Eumeli, Joint Global Ocean Flux Study-France, Villefranche-sur-Mer. 1995.

Legeleux, F., Relations entre particules marines et message sédimentaire: Flux de matière dans la colonne d'eau et transformations à l'interface eau-sédiment dans l'océan tropical du nord-est, Thèse de doctorat, Paris 6, 1994.

Legeleux, F., J.-L. Reyss, H. Etcheber, and A. Khripounoff, Fluxes and balance of ^{210}Pb in the tropical northeast Atlantic, *Deep Sea Res. Part I, 43*, 1321-1341, 1996.

Lepple, F.K., and C.J. Brine, Organic constituents in eolian dust and surface sediments from northwest Africa, *J. Geophys. Res., 81*, 1141-1147, 1976.

Levitus, S., Climatological atlas of the world ocean, *NOAA Prof. Pap., 13*, 173, 1982.

Li, X., H. Maring, K. Voss, and J.M. Prospero, Dominance of mineral dust in aerosol light-scattering in the North Atlantic trade winds, *Nature, 380*, 416-419, 1996.

Martin, J.H., S.E. Fitzwater, and R.M. Gordon, Iron deficiency limits primary production in Antarctic waters, *Global Biogeochem. Cycles, 4*, 5-12, 1990.

Michaels, A.F., M.W. Silver, M.M. Gowing, and G.A. Knauer, Cryptic zooplankton "swimmers" in the upper ocean sediment traps, *Deep Sea Res., 37*, 1285-1296, 1990.

Mittelstaedt, E., The ocean boundary along the northwest African coast: Circulation and oceanographic properties at the sea surface, *Prog. Oceanogr., 26*, 307-355, 1991.

Morel, A., An ocean flux study in eutrophic, mesotrophic and oligotrophic situations: The EUMELI program, *Deep Sea Res. Part I, 43*, 1185-1190, 1996.

Morel, A., D. Antoine, M. Babin, and Y. Dandonneau, Measured and modeled primary production in the northeast Atlantic (EUMELI JGOFS program): The impact of natural variations in photosynthetic parameters on model predictive skill, *Deep Sea Res. Part I, 43*, 1273-1304, 1996.

Mortlock, R.A., and P.N. Froelich, A simple method for the rapid determination of biogenic opal in pelagic marine sediments, *Deep Sea Res., 36*, 1415-1426, 1989.

Moulin, C., F. Guillard, F. Dulac, and C.E. Lambert, Long-term daily monitoring of Saharan dust load over marine areas using Meteosat ISCCP-B2 data, 1, Methodology and preliminary results for 1983-1994 in the Mediterranean, *J. Geophys. Res., 102*, 16,947-16,958, 1997a.

Moulin, C., C.E. Lambert, F. Dulac, and U. Dayan, Control of atmospheric export of dust from North Africa by the North Atlantic Oscillation, *Nature, 387*, 691-694, 1997b.

Neuer, S., V. Ratmeyer, R. Davenport, G. Fischer, and G. Wefer, Deep water particle flux in the Canary Island region: Seasonal trends in relation to long-term satellite derived pigment data and lateral sources, *Deep Sea Res. Part I, 44*, 1451-1466, 1997.

Newton, P.P., R.S. Lampitt, T.D. Jickells, P. King, and C. Boutle, Temporal and spatial variability of biogenic particle fluxes during the JGOFS northeast Atlantic process studies at 47°N, 20°W, *Deep Sea Res. Part I, 41*, 1617-1642, 1994.

Pierre, C., A. Vangriesheim, and E. Laube-Lenfant, Variability of water masses and of organic production-regeneration systems as related to eutrophic, mesotrophic and oligotrophic conditions in the northeast Atlantic Ocean, *J. Mar. Syst., 5*, 159-170, 1993.

Pilskaln, C.H., and S. Honjo, The fecal pellet fraction of biogeochemical particle fluxes to the deep sea, *Global Biogeochem. Cycles, 1*, 31-48, 1987.

Prospero, J.M., The atmospheric transport of particles to the ocean, in *Particle Flux in the Ocean*, SCOPE report vol. 57, edited by V. Ittekkot et al., pp. 19-52, John Wiley, New York, 1996a.

Prospero, J.M., Saharan dust transport over the North Atlantic Ocean and Mediterranean: An overview, in *The Impact of Desert Dust From Northern Africa Across the Mediterranean*, edited by S. Guerzoni and R. Chester, pp. 133-151, Kluwer Acad., Norwell, Mass., 1996b.

Prospero, J.M., and T.N. Carlson, Vertical and areal distribution of Saharan dust over the western equatorial North Atlantic Ocean, *J. Geophys. Res., 77*, 5255-5265, 1972.

Prospero, J.M., and R.T. Nees, Dust concentration in the atmosphere of the equatorial North Atlantic: Possible relationship to the Sahelian drought, *Science, 196*, 1196-1198, 1977.

Ratmeyer, V., G. Fischer, and G. Wefer, Lithogenic particle fluxes and grain size distributions in the deep ocean off NW Africa: Implications for seasonal changes of aeolian dust input and downward transport, *Deep Sea Res. Part I, 46*, 1289-1337, 1999.

Rea, D., The paleoclimatic record provided by eolian deposition in the deep sea: The geologic history of wind, *Rev. Geophys., 32*, 159-195, 1994.

Savoie, D.L., and J.M. Prospero, Aerosol concentration statistics for the northern tropical Atlantic, *J. Geophys. Res., 82*, 5954-5964, 1977.

Schulz, M., Y. Balkanski, W. Guelle, and F. Dulac, Role of aerosol size distribution and source location in a three–dimensional simulation of a Saharan dust episode tested against satellite–derived optical thickness, *J. Geophys. Res., 103*, 10,579-10,592, 1998.

Schütz, L., Long range transport of desert dust with special emphasis on the Saharan desert, *Ann. NY. Acad. Sci., 338*, 515-532, 1980.

Scientific Committee on Oceanic Research, Core measurement protocols: Report of the core measurements working groups, *JGOFS Rep. 6*, Halifax, N.S., Canada, 1990.

Semmelhack, W., Die staubfälle im nordwestafrikanischen gebiet des Atlantischen ozeans, *Ann. Hydrogr., 62*, 273-277, 1934.

Shimmield, G., Cruise report, R.R.S. *Charles Darwin 53*, BOFS 1990 Leg C, Univ. of Edinburgh, Edinburgh, Scotland, 1990.

Siegel, D.A., and W.G. Deuser, Trajectories of sinking particles in the Sargasso Sea: Modeling of statistical funnels above deep–ocean sediment traps, *Deep Sea Res. Part I, 44*, 1519-1541, 1997.

Siegel, D.A., T.C. Granata, A.F. Michaels, and T.D. Dickey, Mesoscale eddy diffusion, particle sinking, and the interpretation of sediment trap data, *J. Geophys. Res., 95*, 5305-5311, 1990.

Speth, P., and H. Detlefsen, Meteorological influences on upwelling off Northwest Africa, *Rapp. P. V. Réun. Cons. Int. Explor. Mer., 180*, 29-34, 1982.

Stramma, L., and G. Siedler, Seasonal changes in the North Atlantic subtropical gyre, *J. Geophys. Res., 93*, 8111-8118, 1988.

Swap, R., M. Garstang, S. Greco, R. Talbot, and P. Kållberg, Saharan dust in the Amazon Basin, *Tellus, 44B*, 133-149, 1992.

Swap, R., S. Ulanski, M. Cobbett, and M. Garstang, Temporal and spatial characteristics of Saharan dust outbreaks, *J. Geophys. Res., 101*, 4205-4220, 1996.

Tachikawa, K., C. Jeandel, A. Vangriesheim, and B. Dupré, Distribution of rare earth elements and neodymium isotopes in suspended particles of the tropical Atlantic Ocean (EUMELI site), *Deep Sea Res. Part I, 46*, 733-755, 1999.

Taylor, S.R., and S.M. McLennan, *The Continental Crust: Is Composition and Evolution*, Blackwell, Malden, Mass., 1985.

Tegen, I., A.A. Lacis, and I. Fung, The influence on climate forcing of mineral aerosols from disturbed soils, *Nature, 380*, 419-422, 1996.

Turekian, K.K., and K.H. Wedepohl, Distribution of the elements in some major units of the Earth's crust, *Geol. Soc. Am. Bull., 72*, 175-192, 1961.

van Camp, L., L. Nykjær, E. Mittelstaedt, and P. Schlittenhardt, Upwelling and boundary circulation off Northwest Africa as depicted by infrared and visible satellite observations, *Prog. Oceanogr., 26*, 357-402, 1991.

Vangriesheim, A., C. Pierre, and E. Laube, Hydrological conditions in the EUMELI area in the NE tropical Atlantic: Water masses, variability of productivity/regeneration and of particle load, *Ann. Inst. Océanogr., 69*, 15-20, 1993.

Vinogradov, A.P., *The Geochemistry of Rare and Dispersed Chemical Elements in Soils*, Consult. Bur., New York, 1959.

Walsh, I., J. Dymond, and R. Collier, Rates of recycling of biogenic components of settling particles in the ocean derived from sediment trap experiments, *Deep Sea Res., 35*, 43-58, 1988.

Wollast, R., Evaluation and comparison of the global carbon cycle in the coastal zone and in the open ocean, in *The Sea*, vol. 10, *The Global Coastal Ocean: Regional Studies and Syntheses*, edited by A. R. Robinson and K.H. Brink, pp. 213-252, John Wiley, New York, 1998.

Zenk, W., B. Klein, and M. Schröder, Cape Verde frontal zone, *Deep Sea Res., 38*, 505-530, 1991.

Zhuang, G., and R.A. Duce, The adsorption of dissolved iron on marine aerosol particles in surface waters of the open ocean, *Deep Sea Res. Part I, 40*, 1413-1429, 1993.

A. J.-M. Bory, Lamont-Doherty Earth Observatory of Columbia University, P.O. Box 1000, Route 9W, Palisades, NY 10964-8000. (bory@ldeo.columbia.edu)

P. P. Newton, School of Biological and Molecular Sciences, Oxford Brookes University, Gipsy Lane, Headington, Oxford OX3 0BP, United Kingdom.

(Received April 21, 1999; revised September 13, 1999;
accepted September 16, 1999.)